ORIGINAL RESEARCH ARTICLE

Vadose Zone Journal OPEN ACCESS

Dynamic groundwater recharge simulations based on cosmic-ray neutron sensing in a tropical wet experimental basin

Luís Romero Barbosa[1,2,3] | **Victor Hugo R. Coelho**[4] | **Lena M. Scheiffele**[1] | **Gabriele Baroni**[5] | **Geraldo M. Ramos Filho**[2] | **Suzana M. G. L. Montenegro**[3] | **Cristiano das N. Almeida**[2] | **Sascha E. Oswald**[1]

[1] Institute of Environmental Science and Geography, Univ. of Potsdam, Karl-Liebknecht-Str. 24-25, Potsdam, 14476, Germany

[2] Dep. of Civil and Environmental Engineering, Federal Univ. of Paraíba, Cidade Universitária, João Pessoa, Paraíba 58051-900, Brazil

[3] Dep. of Civil Engineering, Federal Univ. of Pernambuco, Recife, Brazil

[4] Dep. of Geosciences, Federal Univ. of Paraíba, João Pessoa, Brazil

[5] Dep. of Agricultural and Food Sciences, Univ. of Bologna, Viale Fanin 50, Bologna, Italy

Correspondence
Sascha E. Oswald, Institute of Environmental Science and Geography, Univ. of Potsdam, Karl-Liebknecht-Str. 24-25, Potsdam, Germany, 14476.
Email: sascha.oswald@uni-potsdam.de

Assigned to Associate Editor Karsten Jensen.

Abstract

Although cosmic-ray neutron sensing (CRNS) is probably the most promising noninvasive proximal soil moisture measurement technique at the field scale, its application for hydrological simulations remains underexplored in the literature so far. This study assessed the use of CRNS to inversely calibrate soil hydraulic parameters at the intermediate field scale to simulate the groundwater recharge rates at a daily timescale. The study was conducted for two contrasting hydrological years at the Guaraíra experimental basin, Brazil, a 5.84-km², a tropical wet and rather flat landscape covered by secondary Atlantic forest. As a consequence of the low altitude and proximity to the equator low neutron count rates could be expected, reducing the precision of CRNS while constituting unexplored and challenging conditions for CRNS applications. Inverse calibration for groundwater recharge rates was used based on CRNS or point-scale soil moisture data. The CRNS-derived retention curve and saturated hydraulic conductivity were consistent with the literature and locally performed slug tests. Simulated groundwater recharge rates ranged from 60 to 470 mm yr^{-1}, corresponding to 5 and 29% of rainfall, and correlated well with estimates based on water table fluctuations. In contrast, the estimated results based on inversive point-scale datasets were not in alignment with measured water table fluctuations. The better performance of CRNS-based estimations of field-scale hydrological variables, especially groundwater recharge, demonstrated its clear advantages over traditional invasive point-scale techniques. Finally, the study proved the ability of CRNS as practicable in low altitude, tropical wet areas, thus encouraging its adoption for water resources monitoring and management.

Abbreviations: COSMIC, COsmic-ray Soil Moisture Interaction Code; cph, counts per hour; CRNS, cosmic-ray neutron sensing; GEB, Guaraíra experimental basin; KGE, Kling–Gupta efficiency; MRC, Master Recession Curve; PR2, profile probe; RWU, root water uptake; TDR, time-domain reflectometry; WTF, water table fluctuation

1 | INTRODUCTION

Groundwater recharge is a complex ecohydrological process that plays an important role to societies as a key strategic water reserve (Wada et al., 2014), and within the environments

as a natural or artificial mechanism of groundwater storage renewal (Gleeson et al., 2012). The groundwater recharge connects the atmospheric, surface, and subsurface components of the water balance (Mohan et al., 2018), being mainly controlled by the precipitation amount and intensity, boundary layer climatology, topography, water table level, watershed geomorphology, soil and vegetation characteristics, and irrigation return flow (Jasechko et al., 2014; Moeck et al., 2020). Understanding the seasonal controls upon recharge requires its accurate estimation (Jasechko et al., 2014), which can only be obtained by experimental methods or modelling since the groundwater recharge cannot be directly measured (Melo et al., 2015).

A considerable range of experimental methods and models is available for groundwater recharge estimation at various spatiotemporal scales, whose correct selection depends on data availability, desired spatiotemporal resolution, and result representations (Walker et al., 2019). Amongst the existing approaches, the following methods are frequently used to estimate groundwater recharge: (a) monitoring of groundwater level in unconfined aquifers, such as the water table fluctuation (WTF) method (Cai & Ofterdinger, 2016; Wendland et al., 2007); (b) tracer techniques, which estimate aquifer renewal through the concentrations of chemical elements and substances in the water, such as the chloride mass-balance method (Brunner et al., 2004; Hornero et al., 2016); (c) the water balance method, which uses the main components of the water cycle as inputs and outputs of the system (Hornero et al., 2016; Wendland et al., 2007); Darcy's law application, which uses the hydraulic gradient and conductivity to calculate the soil water percolation rates (Callahan et al., 2012; Yin et al., 2011); and (d) numerical modeling, which consists of a mathematical representation of the groundwater processes (Melo et al., 2015; Šimůnek, 2015).

The vertical percolation rate from the numerical simulation of the vadose zone is often considered as a proxy of groundwater recharge (Mathias et al., 2017). The simulation of these groundwater fluxes, however, come with the necessity of the proper calibration of some soil hydraulic parameters by means of soil moisture observations (Graham et al., 2018).

Three different basic approaches are currently available for retrieving soil moisture information: in situ measurements, remote sensing data, and proximal soil sensing. In situ measurements are generally the most accurate and direct methods for collecting soil moisture data but provide point-scale information only, whereas spatially extended information demands time-consuming and burdensome efforts, as the case for wireless sensor networks (Bogena et al., 2010) or spatial time-domain reflectometry (TDR) probes (Graeff et al., 2010). Satellite-borne remote sensing products feature a large-scale estimation of soil moisture (e.g., through active microwave sensors), but usually provide near-surface or root-zone information with coarse spatiotemporal resolutions (Famiglietti

---

Core Ideas

- Cosmic-ray neutron sensing (CRNS) can detect field-scale soil moisture also at low latitudes.
- Soil hydraulic parameters were calibrated using CRNS and inverse simulations.
- Daily groundwater recharge rates were simulated using CRNS-based soil hydraulic parameters.
- CRNS-based recharge was matching independent area average recharge estimates.

---

et al., 2015). Lastly, proximal soil sensing methods became a promising alternative method to monitor soil moisture noninvasively and at the field scale (Bogena et al., 2015; Robinson et al., 2008) based on the relationship from targeted relevant subsurface variables (e.g., groundwater table) to soil properties that could relatively easily be mapped from the surface. Amongst them, the cosmic-ray neutron sensing (CRNS) method (Zreda et al., 2008) is currently the most promising technique, closing the inconvenient spatial scale gap between invasive sensor data and satellite-based remote sensing products. The CRNS uses the inverse relationship between above-ground neutron count rate and all close-by hydrogen content pools (Desilets et al., 2010; Hendrick & Edge, 1966). It continuously measures average soil moisture from about 130-to-240-m effective radius and from about 15-to-55-cm penetration depth for wet and dry conditions, respectively (Köhli et al., 2015; Schrön et al., 2017). Another advantage of CRNS includes the calibration dependence on a single site-specific parameter through a standard curve.

During the last decade, several studies applied and progressed the CRNS method on stationary and mobile platforms up to the scale of square kilometers (Fersch et al., 2020; Schrön, Rosolem, et al., 2018) and by monitoring stations installed in a broad variety of climate conditions—namely, continental (Baatz et al., 2014), temperate (Evans et al., 2016), semiarid (Zreda et al., 2012), and tropical (Hawdon et al., 2014). The CRNS was further successfully applied in vegetated areas such as cropped fields (Franz, reda, Rosolem, et al., 2013; Rivera Villarreyes et al., 2011) and forests (Bogena et al., 2013; Heidbüchel et al., 2016). Most CNRS studies presented good performances when compared with soil moisture datasets from gravimetric experiments, invasive point-scale probes, and land surface models. The advantages of the CNRS method have boosted its application (Franz et al., 2020) in various scientific topics, like runoff dynamics (Dimitrova-Petrova et al., 2020), snow dynamics (Schattan et al., 2017), canopy water interception (Baroni & Oswald, 2015), vegetation biomass calculation (Franz, Zreda, Rosolem, et al., 2013), remotely sensed products validation (Montzka et al., 2017),

land surface modeling (Baatz et al., 2017), agricultural support and irrigation (Finkenbiner et al., 2018; Li et al., 2019), and urban effects (Schrön, Zacharias, et al., 2018).

Although there is a variety of CRNS studies, the assessment of its performance and application remains poorly explored in regions that gather unfavorable environmental conditions for CRNS operation (Bogena et al., 2013). One of the more unfavorable conditions can be found in tropical regions that often exhibit: (a) a high geomagnetic cutoff rigidity, which reduces the secondary cosmic-ray intensities and thus incoming neutron intensities (Andreasen et al., 2017); (b) the tropical rainforest, whose higher atmospheric humidity and biomass content decrease the possibilities of aboveground neutron detection (Baatz et al., 2015; Jakobi et al., 2018; Köhli et al., 2021); and (c) high soil moisture values shrinking the CRNS support volume (penetration depth and horizontal footprint). Due to these unfavorable conditions, the CRNS data have been very rarely studied in tropical regions, an exemption being (Hawdon et al., 2014) in Northern Australia, whose information has been used for space-borne satellite product validation (Duygu & Akyürek, 2019; Montzka et al., 2017) and model calibration (Shuttleworth et al., 2013). The potential of CRNS for deriving also groundwater recharge rates has been suggested (Baroni et al., 2012), but not specifically targeted so far.

Few studies have used CRNS data to derive soil hydraulic parameters in combination with orthogonal functions (Finkenbiner et al., 2018; Gibson & Franz, 2018), in inverse modeling (Rivera Villarreyes et al., 2014), and also in combination with neutron transport models (Baatz et al., 2017). The COsmic-ray Soil Moisture Interaction Code (COSMIC) developed by Shuttleworth et al. (2013) provided a simplified physically based analytical approach that reduces the computational cost of neutron transport simulations for the inverse calibration of soil hydraulic parameters. Recently, it was efficiently coupled with the one-dimensional soil hydrological model HYDRUS-1D, enabling its use for vadose zone simulations at intermediate field scales (Brunetti et al., 2019).

Based on this knowledge, this study assesses the use of non-invasive CRNS data for two contrasting hydrological years to inversely calibrate the soil hydraulic parameters at intermediate field scale and, with this information, simulating the dynamic groundwater recharge rates through the physically based soil hydrological model HYDRUS-1D (Šimůnek et al., 2016). The hydrological simulation of quantities in the vadose zone based on the CRNS data (i.e., soil moisture, soil hydraulic properties, and groundwater recharge) were tested against additional measurements and compared with the results obtained using point-scale conventional time series (e.g., TDR probes). The experimental site of this study holds unfavorable conditions for CRNS operation with its location close to the equator, low-altitude tropical wet climate, and shallow groundwater table and thus fills a gap within CRNS studies worldwide. In this study, we hypothesized that the use of CRNS data for estimating hydrological variables, also in such regions, will result in a higher prediction accuracy than the traditionally applied invasive point-scale techniques.

2 | MATERIALS AND METHODS

2.1 | Study area and monitoring network

This study was carried out in the Guaraíra experimental basin (GEB, Figure 1), located between the coordinates 07°16′35″–07°19′11″ S and 35°01′18″–35°02′27″ W, which is operated as part of the Brazilian Hydrology Network for the Semi-Arid Region (REHISA) since 2003. The GEB is located at ∼25 km from the shoreline from northeastern Brazil, situated on the surrounding rural area of João Pessoa city (Paraíba state's capital). The GEB comprises a total area of 5.84 km² with a mean elevation of 100 m asl and a rather flat landscape with a mean slope equal to 1.8%. The GEB lies within the Gramame river basin that is the topic of recent investigations, also in respect to larger-scale estimations of groundwater recharge from satellite remote sensing (Barbosa, 2020). The Gramame river basin has a mean potential groundwater availability of ∼1.07 × 10⁸ m³ yr⁻¹, whereas the cumulative withdrawals sum up already to 83.9%, much larger than the maximum recommended exploitation of 60% (PERH-PB, 2006). The groundwater recharge in the region is mainly promoted by vertical infiltration (i.e., diffuse recharge) over these sedimentary terrains.

The GEB features a tropical wet climate with dry summer and well-distinguished rainy season during the austral autumn and winter (As), according to the Köppen climate classification (Alvares et al., 2013). The rainfall in the region is mainly formed from shallow convective clouds, with a mean annual rainfall of 1,700 mm, ∼70% of which occurs from March to July. The air temperature and potential evapotranspiration are high in the experimental basin, with mean annual values of approximately 25.4 °C and 1,500 mm, respectively. The predominant land use and land cover in GEB are forest (native and secondary Atlantic remnants), cropland (sugarcane [*Saccharum* spp.] and pineapple [*Ananas comosus* (L.) Merr.]), and built-up areas (rural housing and unpaved roads). The soil in GEB originated from crystalline basement erosion during the Late Quaternary, which constitutes massive deposits of friable sands (Rossetti et al., 2012). The soil texture in the experimental basin is mainly composed of coarse sand (∼46%), fine sand (∼52%), and silt and clay (∼2%), belonging to the haplic acrisol and carbic podzol soil types encompassing the study area (Barbosa et al., 2019; IUSS Working Group WRB, 2015).

The study used data from two monitoring sites in GEB (S1 and S2, Figure 1), the vegetation at these sites being
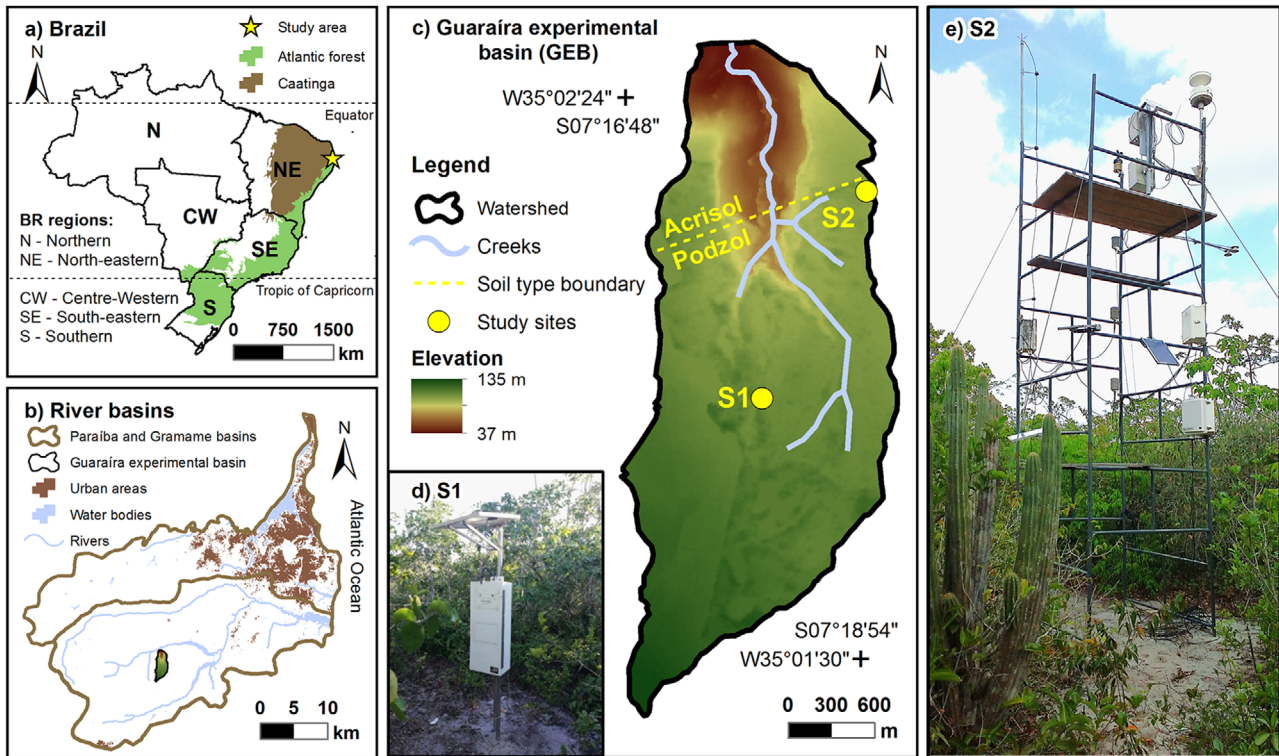
FIGURE 1 Representation of (a) Brazil (BR), (b) Paraíba and Gramame river basins with João Pessoa city, (c) Guaraíra experimental basin, (d) location S1 with a cosmic-ray neutron sensing probe, and (e) location S2 with a meteorological station including a time-domain reflectometry soil moisture profile

sparse tropical forest of 3-to-4-m height in secondary-growth stage with no substantial litter layer to observe. The sites were equipped with rain gauges, meteorological sensors (e.g., radiometer, anemometer, and thermo-hygrometer), invasive and noninvasive soil moisture probes, and groundwater monitoring wells. One noninvasive CRNS probe was installed at S1 for recording hourly soil moisture values. On its surrounding, three soil profile probes type PR2 (Delta-T Device) were vertically inserted into the soil at radial distances of 17, 66, and 153 m from the CRNS probe, for monitoring the hourly soil moisture in the depths of near-surface in 10, 20, 30, 40, 60, and 100 cm. The generalized polynomial calibration curve optimized by the PR2 manufacturer was used, as it covers a wide range of mineral soil types with organic content of ∼1% (Delta-T, 2016), which is the case at GEB. Hardware problems have made the measured data in depths >10 cm unreliable for two profile probes, whereas only the one at 66-m distance to the CRNS sensor delivered reliable values for all depths during the entire observation period. For testing the CRNS derived soil moisture, the soil moisture time series monitored in the near surface (10-cm depth) by the three PR2 profile probes were smoothed through a moving average and integrated to an area average soil moisture using the weighting function (Schrön et al., 2017). Three invasive soil moisture sensors (Campbell Scientific, CS616 water content reflectometer) were horizontally inserted in the soil at S2 to monitor a profile of soil moisture in the depths of 5, 20, and 40 cm, recorded also at hourly timescale. The measurement principle is based on a transmission line oscillator and works similar to TDR systems (Blonquist et al., 2005) and for simplicity the sensors will be called TDR probes within this study. Groundwater levels were recorded using fast-response pressure transducers. The groundwater table depth in GEB showed a mean value of ∼157 cm below the surface, influenced by the shallow occurrence of a Si-cemented impermeable layer in the mean depth of ∼200 cm below the surface. All the datasets were averaged in this study to values at daily timescale. We assume similar hydrologic behavior at the sites S1 and S2, based on the measured data on texture and bulk density, which is confirmed by measurements from Santos et al. (2012), who reported extensive measurements of soil characteristics and hydrological properties within the catchment (raw data can be obtained from the appendix of Silva (2009).

Figure 2 shows the usage of the data within this study at each field site and comparisons drawn between datasets and field sites. Firstly, the CRNS calibration based on gravimetric soil sampling and a comparison with independent soil moisture profile measurements (PR2) is intended to test the usability of CRNS as soil moisture monitoring method in humid tropic conditions. Secondly, after this basic validation of CRNS applicability, the time series of corrected neutron count rates is used directly to inversely estimate the soil hydraulic
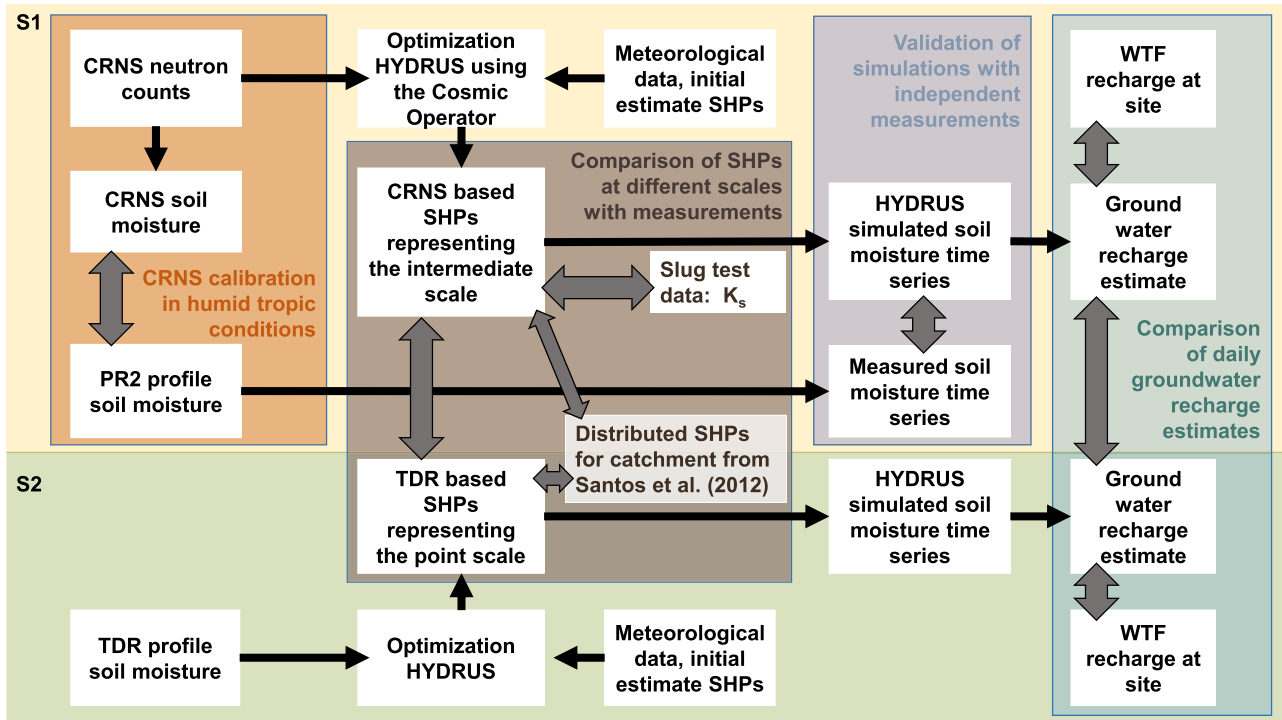
FIGURE 2 Workflow (black arrows) showing the different measurement setups at the two locations used within this study (S1 = top and S2 = bottom). Comparisons between data products are marked with a gray, two-sided arrow. A device for cosmic-ray neutron sensing (CRNS) was calibrated at S1 and its applicability in humid tropic conditions was validated by independent soil moisture profile measurements (PR2). Soil hydraulic parameters (SHPs) were optimized independently within HYDRUS at each field site (CRNS and Cosmic Operator at S1, using a time-domain reflectometry [TDR] soil moisture probes at S2), derived parameters were compared with values from literature and a slug test validated the saturated hydraulic conductivity (K_s) at S1. The CRNS-based simulated soil moisture time series at S1 were validated by independent measurements (PR2). Based on the simulated fluxes at S1 and at S2, at each site a time series of groundwater recharge estimates was obtained and compared to independent estimates derived from water table fluctuation (WTF) measured in groundwater wells

parameters within HYDRUS 1D coupled with the COSMIC operator (Brunetti et al., 2019). The resulting fluxes due to the nature of the CRNS data represent effective field-scale estimates. Thirdly, a standard approach for inverse calibration of the hydraulic parameters using soil moisture time series (TDR) is applied at S2, representing point-scale parameters. Fourthly, the calibrated parameter sets of both locations were compared with data reported in literature (Santos et al., 2012) reflecting the variability observed within the catchment. Saturated hydraulic conductivity based on CRNS data was independently validated with slug tests at S1. Moreover, the simulated soil moisture time series resulting from the CRNS-optimized parameter set at S1 is compared with the independent profile soil moisture of the PR2. Finally, the simulated vertical percolation (constituting groundwater recharge) was derived at S1 based on the area average CRNS data and at S2 based on the point-scale TDR data. Both recharge estimates were compared with recharge estimates using fixed-interval WTF from groundwater wells at each site.

2.2 | CRNS data

In this study, a CRNS probe equipped with a ^{3}He neutron counter (manufactured by Hydroinnova, type CRS 1000) was installed at a location seen as typical for GEB conditions to record the neutron count rate at hourly intervals as cumulative neutron counts. Standard correction procedures for atmospheric pressure, incoming neutron count rate and air humidity were applied to the raw neutron count rate (see Appendix A for details).

The theoretical relationship between corrected neutron count rate N' (in counts per hour [cph]) and soil moisture depends on the dry neutron count rate parameter N_0 (in cph) (Desilets et al., 2010; Equation 1). This parameter was calibrated based on soil moisture measured by the gravimetric method on soil samples collected at 17 locations (Figure 3) in three depth intervals (0–5, 5–10, and 15–20 cm), so that different moisture conditions in the CRNS footprint were covered. The weighted average soil moisture using the weighting
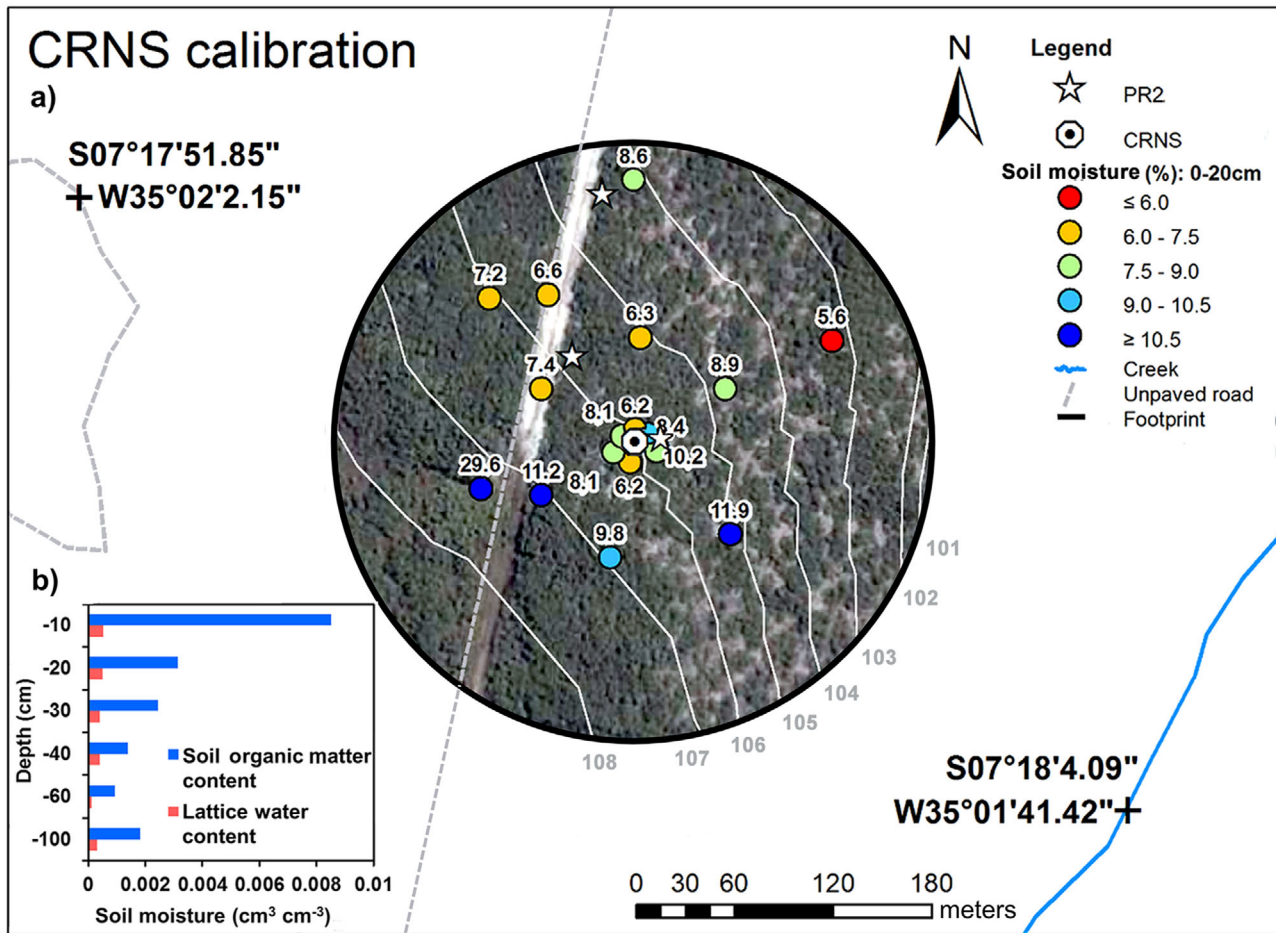
FIGURE 3 Calibration of the cosmic-ray neutron sensing (CRNS). Distribution of (a) the vertically weighted soil moisture around the CRNS probe retrieved from gravimetric sampling, the locations of the PR2 profile probes, and (b) the average water equivalent from soil organic matter and lattice water content per depth. A medium-size footprint of 180-m radius is indicated here for illustration, but it varies between dry and moist environmental conditions to some extent

function proposed by Köhli et al. (2015) was then calculated and used to calibrate the CRNS standard calibration curve. For calculating N_0, the corrected neutron count rate was averaged during the calibration period and used alongside with the weighted average soil moisture and the total bound water content. The latter component corresponds to the sum of soil organic matter and lattice water contents (θ_{SOM} and θ_{LW}, in cm³ cm⁻³), which were calculated in this study according to Heidbüchel et al. (2016), by weighting soil samples after drying at 105 °C for 24 h (m_{105}), and burning 10 g of dry samples at 400 °C for 16 h (m_{400}) and 1,000 °C for 12 h ($m_{1,000}$) (Equations 2 and 3). The soil bulk density (ρ_{bd}) was obtained by averaging the gravimetric-based estimates, and the density of water (ρ_w) was adopted as 1 g cm⁻³.

$$\theta = \left(\frac{0.0808}{N'/N_0 - 0.372} - 0.115 \right) \frac{\rho_{bd}}{\rho_w} - \theta_{SOM} - \theta_{LW} \quad (1)$$

$$\theta_{SOM} = 0.556 \frac{m_{105} - m_{400}}{m_{105}} \rho_{bd} \quad (2)$$

$$\theta_{LW} = \frac{m_{400} - m_{1,000}}{m_{105}} \rho_{bd} \quad (3)$$

The effect of biomass water equivalent was neglected in this study, because forest biomass and litter layer are much smaller than in other CRNS studies (Bogena et al., 2013; Heistermann et al., 2021) and the effect of a tree canopy as an additional moderator and the creation of neutrons with detectable energy ranges are still under discussion (Baroni & Oswald, 2015; Li et al., 2019). The CRNS-based soil moisture determined for hourly integration periods was smoothed to a 24-h timescale (i.e., representing daily values), using the moving average calculation to reduce the stochastic measurement noise caused by

low incoming neutron count rate (Bogena et al., 2013). This is longer than in other studies but related to the high cutoff rigidity close to the equator.

2.3 | Soil hydrological modelling and estimation of soil hydraulic parameters

Understanding of how soil moisture can be affected by land surface water fluxes allows for comprehensively modeling the groundwater recharge (Sadeghi et al., 2018). Simulations of soil moisture and land surface water fluxes were carried out using the HYDRUS-1D model because of the large number of implemented processes, the flexibility for application in different soil water conditions, and the possibility of inverse calibration (Šimůnek et al., 2016). The recent integration of the COSMIC operator enables the proper handling of CRNS data in this context (Brunetti et al., 2019).

The HYDRUS-1D model is capable of solving the governing flow equations for partially-saturated porous media through Richards' nonlinear partial differential equation (Equation 4; Šimůnek et al., 2008).

$$\frac{\partial \theta}{\partial t} = \frac{\partial}{\partial t}\left[K(h)\left(\frac{\partial h}{\partial x} + \cos \beta\right)\right] - S(h) \tag{4}$$

where θ is the soil moisture, h is the water pressure head (or matric potential), t is time, $S(h)$ is the sink term, $K(h)$ is the unsaturated hydraulic conductivity function, and β is the angle between the flow direction and the vertical axis (= 0° for vertical flow, in this study). The lateral flux was neglected in this study because of the high permeability expected from the thick loose sand of the study area, which impairs the modification of the vertical percolation to an inclined direction (Jankowski, 2014). The sink term of Richards' equation refers to the actual root water uptake (RWU$_a$, for details see Appendix B). A rooting depth of 0.70 m was determined by in situ observations. Variable hydro-phenomenological effects were disregarded on the calculation of RWU in GEB due to the negligible temporal variations observed in situ on the rooting depth and root density.

The soil water output is mainly triggered by potential evapotranspiration ET$_p$, which was estimated using the Penman equation (Penman, 1948) modified by (Shuttleworth, 1993). Beer's equation was then used to split the ET$_p$ into potential soil surface evaporation E_p and the transpiration T_p by the Equations 5 and 6 (Sutanto et al., 2012).

$$T_p = ET_p\left(1 - e^{-k \times LAI}\right) \tag{5}$$

$$E_p = ET_p e^{-k \times LAI} \tag{6}$$

These potential components were calculated based on the leaf area index (LAI) (Bastiaanssen et al., 1998; Huete, 1988), which was averaged over GEB using two Moderate Resolution Imaging Spectroradiometer (MODIS) reflectance products (MOD09Q1 and MYD09Q1). The LAI estimate is based on the main land cover of GEB, which was Atlantic secondary forest. The cloud cover effects within the remote sensing products were attenuated by carrying out monthly map compositions by substituting the pixels with disparate LAI values by pixels of other images in the same month (Barbosa, 2020). These equations use the light extinction coefficient k that, in this study, was set equal to 0.463 due to the arboreal-shrub physiognomies of the vegetation that features a generally rounded canopy (Chen et al., 2014; Raoufi & Beighley, 2017), whose average height of 330 cm was determined by in situ observations. The component T_p was then used to estimate RWU$_p$ by subtracting the interception I, which was calculated by an empirical equation presented by Šimůnek et al. (2013).

The actual evaporation E_a and the infiltration F were calculated by the numerical solution proposed by Neuman et al. (1974), which depends on the upper boundary condition. In this study, the upper boundary was set as the atmospheric condition with maximum surface water layer of 2.5 cm similar to (Batalha et al., 2018), which was observed in situ after ponding occurrences. This information was set to obtain the actual net surface water fluxes S_a, calculated as the F minus E_a. The resulting fluxes were accumulated at daily time scale for the hydrological study years and plotted alongside with their annual total proportions in relation to the potential net surface water fluxes S_p, which refers to F minus E_p.

The simulation of water fluxes depends on the proper calibration of soil hydraulic properties (retention and conductivity) and is crucial for consistently simulating the vertical percolation rates under shallow groundwater conditions (Wessolek et al., 2008), such as in GEB. A study comparing four parametrization methods showed that the inverse calibration based on field soil moisture data implemented in the HYDRUS-1D model provided the best water flux predictions (Graham et al., 2018). Therefore, HYDRUS-1D was used in this study for calculating the matric-potential-dependent soil water retention [i.e., $\theta(h)$] and hydraulic conductivity [i.e., $K(h)$] through the Mualem–van Genuchten soil hydraulic model (van Genuchten, 1980), including the option of air-entry detailed by Vogel et al. (2000) (Equations 7–12):

$$\theta(h) = \begin{cases} \theta_r + \dfrac{\theta_m - \theta_r}{[1 + |\alpha h|^n]^m}, & \text{if } h < h_s \\ \theta_s, & \text{else if } h \geq h_s \end{cases} \tag{7}$$

$$K\left(h\right) = \begin{cases} K_{\mathrm{s}} S_{\mathrm{e}}{}^{1}\left[\dfrac{1-F(S_{\mathrm{e}})}{1-F(1)}\right]^{2}, & \text{if } h < h_{\mathrm{s}} \\ K_{\mathrm{s}}, & \text{else if } h \geq h_{\mathrm{s}} \end{cases} \quad (8)$$

where

$$\theta_{\mathrm{m}} = \theta_{\mathrm{r}} + \left(\theta_{\mathrm{s}} - \theta_{\mathrm{r}}\right)\left(1 + |\alpha h_{\mathrm{s}}|^{n}\right)^{m} \quad (9)$$

$$F\left(S_{\mathrm{e}}\right) = \left(1 - S_{\mathrm{e}}^{*1/m}\right)^{m} \quad (10)$$

$$S_{\mathrm{e}}^{*} = \frac{\theta_{\mathrm{s}} - \theta_{\mathrm{r}}}{\theta_{\mathrm{m}} - \theta_{\mathrm{r}}} S_{\mathrm{e}} \quad (11)$$

$$S_{\mathrm{e}}\left(h\right) = \frac{\theta\left(h\right) - \theta_{\mathrm{r}}}{\theta_{\mathrm{s}} - \theta_{\mathrm{r}}} \quad (12)$$

in which $m = (1 - 1/n)$, and $n > 1$. The α is the air entry suction factor, n is the pore size distribution parameter, l is the pore tortuosity and connectivity lumped parameter, θ_{r} is the residual soil moisture, θ_{s} is the saturated soil moisture, and K_{s} is the saturated hydraulic conductivity. This model reduces to the conventional van Genuchten-Mualem equation (van Genuchten, 1980), in the case of $h_{\mathrm{s}} = 0$ (at site S2), leading to $\theta_{\mathrm{m}} = \theta_{\mathrm{s}}$. The air entry ($h_{\mathrm{s}}$) of −2 cm related to factor α was considered (at site S1) for CRNS based calibration to reduce the nonlinearity effect of the hydraulic conductivity function close to saturated conditions (Ries et al., 2015; Vogel et al., 2000). The l factor was assumed as 0.50, as usually adopted in the literature, because of its underexplored effects on simulations (Mualem, 1976; Ventrella et al., 2019; Wang et al., 2009). Amongst the soil hydraulic parameters, the saturated hydraulic conductivity was specifically assessed in this study, since it affects the vertical percolation rates and, in turn, the groundwater recharge and was shown in previous studies to inhibit a high level of uncertainty (Brunetti et al., 2019; Gibson & Franz, 2018). The hydraulic conductivity was experimentally estimated from water-level displacement datasets resulting from the overdamped injection and withdrawal of a slug in a monitoring well at S1. Such a slug test is expressed by an empirical logarithmic equation that considers: (a) the well, perforation, and effective radii; (b) the well filter length and saturation thickness; and (c) the groundwater table dynamic (Bouwer & Rice, 1976). Six slug-in and slug-out attempts were carried out since the adjusted water level showed an uneven recovering to the static level; therefore, the groundwater level was monitored using a fast-response pressure transducer.

The convergence of the soil hydraulic parameters also relies on the proper input of their initial values for the inverse calibration. Thus, the Rosetta Lite v.1.1 module (Schaap et al., 2001), incorporated in the HYDRUS-1D model (Šimůnek et al., 2008), was used to calculate the initial values of the soil hydraulic parameters from soil texture and hydrophysical data. The vertical soil texture down to 100-cm depth was calculated from the mean soil particle distributions determined by sieving (particle size > 0.063 mm) and sedimentation methods (particle size ≤ 0.063 mm). The hydrophysical data were consistent with soil water contents experimentally obtained in pressured chambers for the suctions at 33 and 1,500 kPa.

In this study, all soil hydraulic parameters except for l were calibrated using CRNS neutron count rate information at S1 and using a profile by TDR soil moisture at S2. For handling the CRNS data within the inverse calibration procedure, the physically based and analytic forward neutron operator COSMIC was used (Shuttleworth et al., 2013). It simulateds a neutron count rate based on soil moisture information. Using measured CRNS neutron count rates thus enables to calibrate the effective soil hydraulic parameters at the intermediate scale. COSMIC is capable of representing the (a) exponential reduction of high energy neutron flux towards deeper soil layers, (b) fast neutron generation from high energy neutrons at different depths, and (c) additional depth-dependent reduction of lower energy neutrons before their detection at the soil surface. The COSMIC operator includes the site-independent parameters $L_1 = 162.0$ g cm^{-2}, $L_2 = 129.1$ g cm^{-2}, and $L_4 = 3.16$ g cm^{-2} (Shuttleworth et al., 2013). The COSMIC operator also includes the site-dependent parameters L_3 (g cm^{-2}) and α (cm^{-3} g^{-1}), which are calculated based on the soil bulk density that was averaged in this study down to 20-cm depth and the total bound water content ($\theta_{\mathrm{SOM}} + \theta_{\mathrm{LW}}$). The soil surface high-energy neutron count N_{C} scales the simulated count rate to the observed count rate and was set in this study to 90 by a trial-and-error approach with forward simulations of the HYDRUS-COSMIC model (based on initial estimates of soil hydraulic properties) to derive lowest deviations to the observed neutron count rate. It was additionally validated by the relationship of the N_0 calibration parameter derived by Baatz et al. (2014) and showed reasonable agreement (data not shown). This leaves the same hydraulic parameters to calibrate for using CRNS data or TDR profiles.

2.4 | Groundwater recharge fluxes

The dynamic vertical percolation rates were simulated for the two contrasting hydrological years 2017–2018 (dry) and

2018–2019 (rainy) by computing the cumulative water fluxes in the depths of 20, 30, 40, 60, and 100 cm, and the bottom boundary. These simulations were performed at an daily timescale to avoid the bias caused by the temporal averaging of the meteorological data (Batalha et al., 2018). The dynamic groundwater recharge rates correspond to the vertical percolation rates in the bottom boundary, which was set as the variable groundwater level due to the shallow occurrence of a Si-cemented impermeable layer in 194 cm at S1 and in 215 cm at S2. In this study, a homogeneous soil sandy profile discretised to 389 nodes at S1 and 431 nodes at S2. Homogeneity can be assumed because of the low variation in texture (>96% sand) and organic matter with depth (>2%). The groundwater recharge (R) was calculated by integrating the water flux over time, applying a water budget equation (Equation 13) that includes precipitation (P), l, RWU_a, E_a, runoff (Q), and soil water storage changes (ΔS). The runoff was only observed in few stretches of GEB, wherein flat natural landscape was modified to install gas pipelines or at the more sloped areas closer to the outlet, leading to negligible results found in simulations that were disregarded in the analyses of this study.

$$R = P - I - RWU_a - E_a - Q - \Delta S \qquad (13)$$

The dynamic of groundwater recharge rates simulated by HYDRUS-1D model was validated by assessing the cumulative groundwater recharge rates obtained from experimental estimates calculated by the WTF method (Equation 14). The WTF method was applied for the two monitoring wells present at S1 and S2. For such purpose, an alternative solution was considered due to daily timescale of simulation, which consists of a fixed-interval WTF method that combines two approaches: the so-called RISE and the Master Recession Curve (MRC) procedures (Nimmo et al., 2015). In this study, the RISE and the MRC procedures were used to determine the contributions of the actual groundwater table rise and the potential groundwater decline, respectively. Moreover, the MRC was defined in this study by linear regression over the longer groundwater recession period, differently from Delin et al. (2007). These approaches involve less subjectivity by circumventing the lack of user's judgment expertise since it adopts a fixed-interval frequency in the accurate measurement of groundwater level (Nimmo et al., 2015).

$$R_{WTF} = S_y \frac{\Delta H}{\Delta t} \qquad (14)$$

where R_{WTF} denotes the groundwater recharge estimated using the WTF method, S_y represents the aquifer specific yield coefficient, Δt is the time from the beginning of the

rise to the peak, and ΔH corresponds to the sum of the actual groundwater rise and the potential groundwater decline for the same period, the latter being obtained by extrapolating the recession curve (Jie et al., 2011). The recession curve is the behavior that the groundwater level would have if no elevation in the groundwater level occurred. The S_y values of 0.10, 0.16, and 0.24 obtained by pumping tests over the region were tested and analyzed for comparison purposes since the S_y can change sensibility according to the depth to the groundwater table (Dettmann & Bechtold, 2016). Values of S_y ranging from 0.10 to 0.26 were similarly reported in other unconfined aquifers of northeastern Brazil (Vasconcelos et al., 2010).

2.5 | Performance metrics

In this study, four statistic metrics were selected to assess the performance of the hydrological simulations. The correlation coefficient (CC, Equation 15) and Kling–Gupta efficiency (KGE, Equation 16) were used to describe the relationship and agreement between simulated and observed datasets, respectively. The mean absolute percentage error (MAPE, Equation 17) and the percent bias (PBIAS, Equation 18) were used to describe the error and bias between simulated and observed datasets, respectively. Percentage values of these two metrics were adopted so that a comparative discussion with the literature results can be performed.
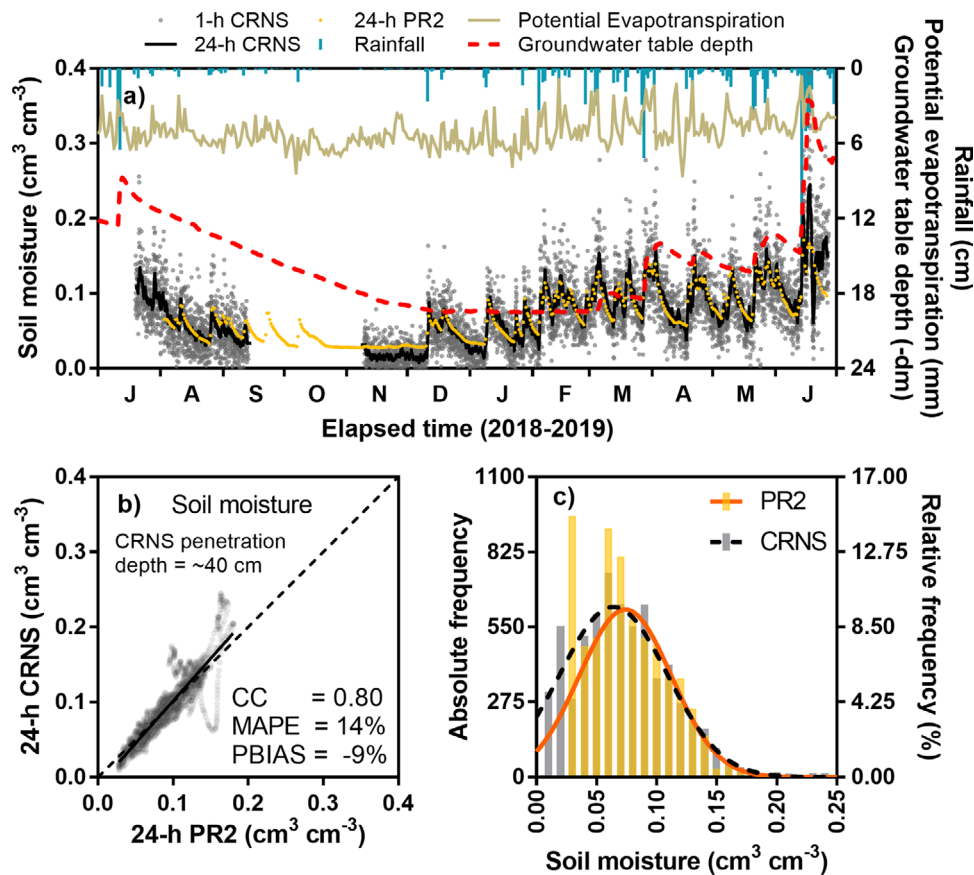
$$CC\,(-) = \frac{\sum_{i=1}^{n} (O_i - \bar{O}) (S_i - \bar{S})}{\sqrt{\sum_{i=1}^{n} (O_i - \bar{O})^2} \sqrt{\sum_{i=1}^{n} (S_i - \bar{S})^2}} \qquad (15)$$

$$KGE\,(-) = 1 - \left[(CC - 1)^2 + \left(\frac{\sigma_S}{\sigma_O} - 1 \right)^2 + \left(\frac{\bar{S}}{\bar{O}} - 1 \right)^2 \right]^{\frac{1}{2}} \qquad (16)$$

$$MAPE\,(\%) = \frac{1}{N} \sum_{i=1}^{n} \left| \frac{O_i - S_i}{O_i} \right| \times 100 \qquad (17)$$

$$PBIAS\,(\%) = \frac{\sum_{i=1}^{n} (S_i - O_i)}{\sum_{i=1}^{n} O_i} \times 100 \qquad (18)$$

where N is the length of a dataset, $\bar{S}$ and $\bar{O}$ are the mean values of the simulated (S_i) and observed (O_i) datasets, respectively, and σ_S and σ_O are the standard deviations of the S_i and O_i datasets, respectively.

FIGURE 4 Comparison between the (a) soil moisture time series based on intermediate-scale cosmic-ray neutron sensing (CRNS) data and average-weighted soil profile probe (PR2) data smoothed by 24-h moving average, with (b) correlation between the CRNS and PR2 data and (c) showing the soil moisture distribution during the observation period. CC, correlation coefficient; MAPE, mean absolute percentage error; PBIAS, percentage bias

3 | RESULTS AND DISCUSSION

3.1 | Calibration of a CRNS sensor under humid tropic conditions

The first set of analyses concerned the calibration of the CRNS, which was operated at S1 to estimate the soil moisture at the intermediate field scale from July 2018 to June 2019 (Figure 3). Gravimetric sampling was performed on 1 Aug. 2018, resulting in the weighted average values of soil moisture and soil bulk density equal to 0.088 $cm^3 \, cm^{-3}$ and 1.11 $g \, cm^{-3}$, respectively, following the weighting procedure outlined in Schrön et al. (2017). Surrounding the CRNS, the soil moisture varied from 0.056 to 0.296 $cm^3 \, cm^{-3}$. The spatial variation was likely influenced by the uneven vegetation cover, implying also an average soil bulk density smaller than that found at four points within the experimental catchment by Barbosa et al. (2019). Additionally, the total bound water content summed up 0.009 $cm^3 \, cm^{-3}$ in the near-surface, which, alongside with soil moisture and soil bulk density, led the dry neutron count rate parameter N_0 to be equal to 550 cph.

Although the total bound water content was relatively small, it was also considered in the CRNS calibration curve for refining the soil moisture estimation, as demonstrated by Baroni et al. (2018).

The resulting daily soil moisture time series consistently responded to the rainfall events and was able to detect the influence of the groundwater level fluctuations during the recession periods (Figure 4). This information was then compared with the PR2 soil moisture time series (weighted area average value using measurements <10-cm depth), showing similar behaviors throughout most of the monitoring period except for the dry season where a slight shift was found. Other studies recommend to calibrate using more than one calibration data set, preferably at different soil moisture stages (Iwema et al., 2015), to improve the calibration result. However, they also adjusted the parameters of the calibration curve to match the independently observed soil moisture. When staying with the standard values of the parameters, deviations in the very wet and dry range of soil moisture were also found by other studies (Baatz et al., 2014; Heidbüchel et al., 2016). Calibration of the parameters and local adjustment of the
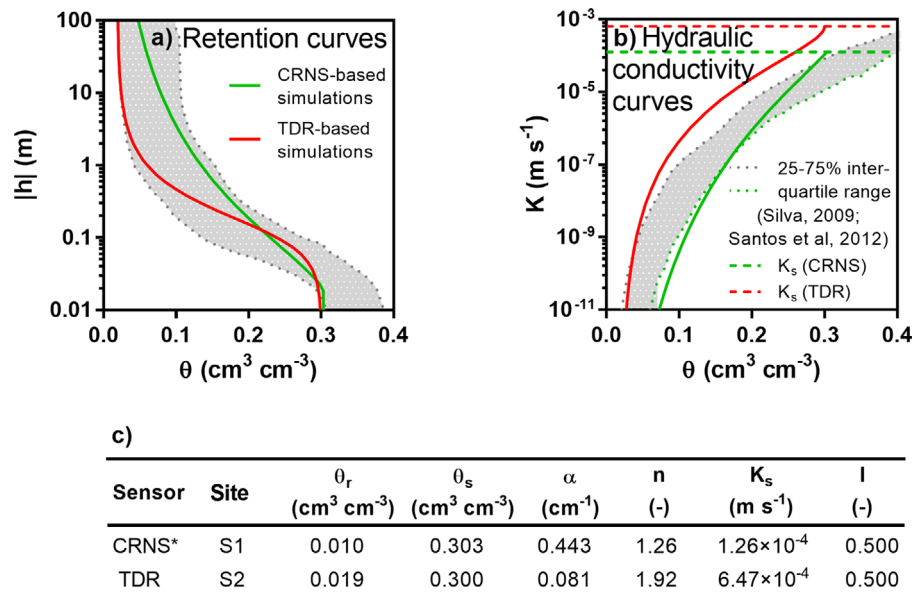
FIGURE 5 Comparison among the (a) retention curves and (b) hydraulic conductivity curves based on (c) the van Genuchten–Mualem parameters (values shown are rounded to the last digit), obtained from time-domain reflectometry (TDR), cosmic-ray neutron sensing (CRNS), and field sampling data (Silva, 2009; Santos et al., 2012). *Adoption of air-entry of −2 cm. K_s, saturated hydraulic conductivity; θ_r, residual soil moisture; θ_s, saturated soil moisture; α, air-entry suction factor; n, pore size distribution parameter; l, pore tortuosity and connectivity lumped parameter

Sensor	Site	θ_r (cm³ cm⁻³)	θ_s (cm³ cm⁻³)	α (cm⁻¹)	n (-)	K_s (m s⁻¹)	l (-)
CRNS*	S1	0.010	0.303	0.443	1.26	1.26×10^{-4}	0.500
TDR	S2	0.019	0.300	0.081	1.92	6.47×10^{-4}	0.500

curve can be a solution to this as demonstrated by Heidbüchel et al. (2016), but was not the goal of this study. Further, a scatter plot between CRNS and PR2 datasets revealed a decent correlation of 0.80 and a tolerable error and underestimation of 14 and −9%, respectively. Moreover, a nearly perfect fit of the linear regression was also found between CRNS and PR2 datasets (slope = 1.13 and y intersect = −0.011 cm³ cm⁻³), even though only PR2 data in <10-cm depth were available to derive the weighted soil moisture. Using a more complete dataset of the soil moisture profile probes, the vertical sensitivity as inherent in CRNS-derived soil moisture could be reduced (Scheiffele et al., 2020). Still, the results in this study show that CRNS can consistently detect soil moisture when operating in humid tropic areas and highlight its potential as a noninvasive soil moisture monitoring method to derive area average soil moisture values.

3.2 | Soil hydraulic parameters

The van Genuchten–Mualem parameters were inversely calibrated from the CRNS neutron count rate data at S1 and based on the TDR-soil moisture data at S2 (Figure 5). Overall, the inverse calibrations provided similar saturated and residual soil moisture values but different shape parameters, showing relatively distinctive retention and hydraulic conductivity curves. The CRNS-based retention was greater than the values derived from the TDR, mainly because of its lower parameter n equal to ~1.26, which reduced the soil hydraulic con-

ductivity, as shown by the lower K_s value of 1.26×10^{-4} m s⁻¹ found S1 in comparison with 6.47×10^{-4} m s⁻¹ found in S2. The K_s values were expected to contain higher uncertainties as the soil saturation during the study site rarely reached saturation (Figure 4). Sales et al. (2014) however, found a mean value of K_s equal to 1.20×10^{-4} m s⁻¹ in forest areas of a representative watershed that encompasses GEB, which is very similar to the CRNS result. Silva (2009) and Santos et al. (2012) conducted a 200-m-mesh experimental study in GEB to obtain soil hydraulic parameters. Their results built the baseline for the water retention and hydraulic conductivity curves and their interquartile range (based on values of $|h|$) as used in this study to compare with the CRNS results. The CRNS-based curves were closer to the interquartile range than the TDR-based curves. Therefore, it was presumed that the soil hydraulic parameters calibrated from the CRNS data were a better match to the area average hydrologic properties.

The difference in hydraulic conductivity curves between the S1 and S2 were, to some extent, the consequence of the different nature of the datasets used to optimize the soil hydraulic parameters (field-scale with CRNS and point-scale with TDR at S1 and S2, respectively). The adoption of the air-entry value of −2 cm for the CRNS-based simulations affects the shape of the curve in the range near saturation (Section 2.3). As the soil moisture rarely approaches saturation (Figure 4) this was expected to be of minor importance on the simulated fluxes from the soil column. On the other hand, the differences between the curves could potentially also be caused by slightly different soil properties at the two locations. To rule
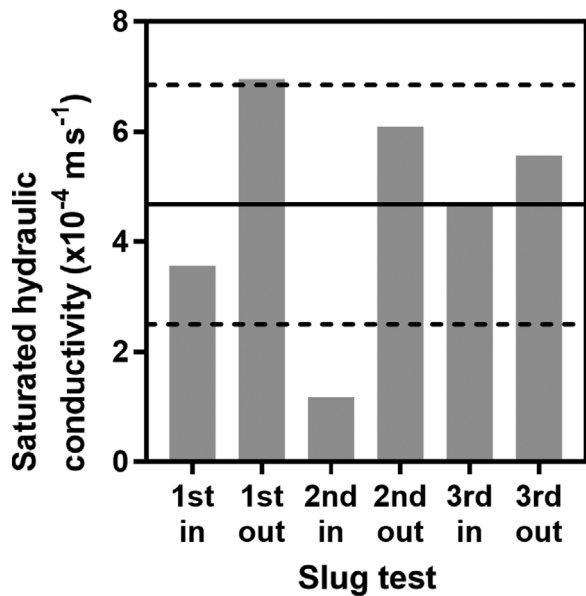
FIGURE 6 Saturated hydraulic conductivity estimated by the slug test. Solid line = mean; dashed line = mean ± standard deviation

out the effect of the location, further validations within this study were thus drawn only between datasets measured at the same site.

Slug tests were carried out in the well at S1 to verify the calibrated values of K_s (Figure 6). The resulting K_s values estimated by the six slug-in and slug-out attempts ranged from 1.18×10^{-4} to 6.96×10^{-4} m s^{-1}, which encompasses the results obtained by inverse calibration from the CRNS as well as from the TDR data. The slug test results thus confirmed the consistency of the inversely calibrated K_s values, matching the soil hydrological characteristics of high permeability in medium clean sand (Cooper et al., 2017; Ishida et al., 2014).

3.3 | Simulated neutron count rate and soil moisture

Aboveground neutron count rate simulated within HYDRUS 1D by the COSMIC operator was plotted against the measured CRNS neutron time series to demonstrate the good fit following the calibration of the soil hydraulic parameters (Figure 7). Overall, COSMIC-based time series adequately responded to the rainfall events, being able to consistently simulate the neutron count rate variability throughout the available data period. This simulated time series tended to slightly underestimate the CRNS neutron count rate particularly during the dry season, likely influenced by the standard parametrization of the calibration curve. The scatter plot between COSMIC and CRNS datasets highlighted the excellent fit of the linear regression (slope = 0.90 and y inter-

sect = 44 cph), as well as a good performance expressed by a high correlation of .89 and an irrelevant mean error of 4% (16 cph). These results confirmed the good performance of the COSMIC operator as found by other studiers, because of its ability to deal with the decreasing sensitivity of CRNS with depth (Baatz et al., 2017; Brunetti et al., 2019; Shuttleworth et al., 2013). The calibrated soil hydraulic parameters enabled the model to simulate the integrated signal from CRNS very well.

To validate the CRNS-based HYDRUS-1D simulation at S1, the simulated soil moisture time series at the depths of 2, 20, 30, 40, 60, and 100 cm is compared to independent soil moisture measurements of PR2 (Figure 8). The results showed that the performance decreases as depth increases, except at the depth of 100 cm, but still providing acceptable levels of correlation varying from .70 to .90 and satisfying linear regression values (slope = 0.58 to 1.23 and y intersect = 0.000 to 0.061 cm^3 cm^{-3}). Conversely, the accuracy was particularly low at -40 cm, showing overestimation of 36% and mean error of 44%, where the greatest leaching through the soil was observed. The overall decreasing correlation of CRNS to soil moisture with increasing depth is in alignment with observations from previous studies (Brunetti et al., 2019; Rosolem et al., 2014) and could be caused by several factors. Most obvious reason is the higher sensitivity of CRNS recordings to the shallower soil layers (Franz, Zreda, Ferre, & Rosolem, 2013; Lv et al., 2014). When comparing CRNS-derived soil moisture to profile measurements, usually stronger dynamics are observed in CRNS soil moisture (compare also Figure 4). Recent studies suggested the application of a profile shape correction, to reduce the inherent vertical sensitivity of the CRNS (Scheiffele et al., 2020), and thus possibly the discrepancy to other measurements with increasing depth, but is still subject of ongoing research. The observed deviation in correlation might also be in parts the consequence of measurements uncertainties at this depth. Finally, since only one profile probe was used (section 2.1), the deviations could also be the result of differences in investigation volume, i.e. the footprint.

After optimizing the soil hydraulic properties based on CRNS data, the integrated signal was reproduced very well (Figure 7) but also the simulated time series show a more immediate response to the rainfall events (Figure 8). Overall, the results showed that the CRNS based simulations were able to consistently simulate the soil moisture responses to rainfall events throughout most of the soil profile.

3.4 | Land surface water fluxes and groundwater recharge

Simulated soil water fluxes at S1 and S2 were analyzed by the cumulative water fluxes of the RWU, evaporation, and
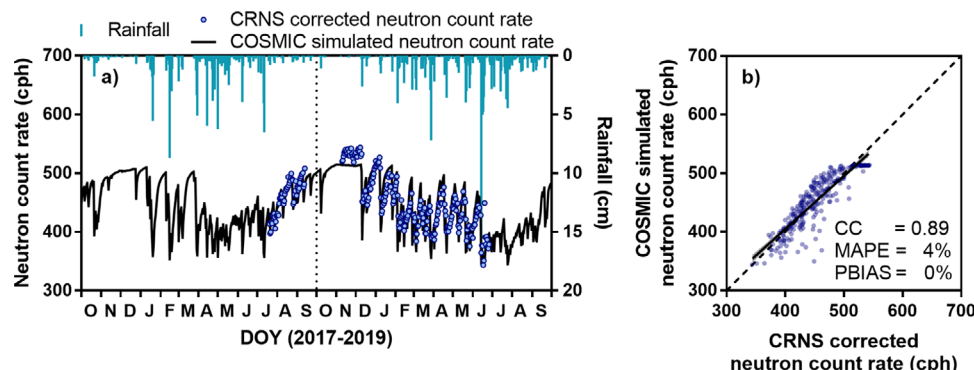
FIGURE 7 Comparison between the (a) neutron count rate simulated by the COsmic-ray Soil Moisture Interaction Code (COSMIC) and the cosmic-ray neutron sensing (CRNS)-corrected neutron count rate, with (b) correlation of between the COSMIC simulated and CRNS corrected count rates. DOY, day of year; CC, correlation coefficient; MAPE, mean absolute percentage error; PBIAS, percentage bias

net surface fluxes (Figure 9). Ratios of actual to potential annual fluxes revealed pertinent spatial changes over GEB, since such ratios of RWU and evaporation remained on ~64 and 63% at S1 and were ~54 and 44% at S2, respectively. These differences were likely caused by the wetter soil condition at S1, as result from its shallower groundwater table since the capillary fringe rise exert a stronger influence on plant transpiration (Han et al., 2015). The actual RWU values were slightly greater than actual evaporation values, likely due to the high net surface fluxes (infiltration minus evaporation), whose actual-to-potential ratio remained on ~89% at S1, and ~84% at S2. These net surface fluxes were similar between S1 and S2 despite a higher hydraulic conductivity found at S2 (see Figure 5). Annual actual evapotranspiration rates from the CRNS-based simulation at S1 are 1,117 and 1,039 mm for 2017–2018 and 2018–2019, respectively. This is close to the mean annual evapotranspiration rate for Atlantic Forest that were estimated using distributed data (MOD16, MODIS Global Evapotranspiration Project) ranging from 1,161 to 1,389 mm (Barbosa, 2020; Cristiano et al., 2015; de Oliveira et al., 2016). The TDR-based simulations at S2 resulted in much lower and less realistic values of 877 and 884 mm.

The simulated effects of the rain events on percolation and groundwater fluxes at S1 and S2 are shown in Figure 10. Due to the shallow groundwater table at GEB, the recharge can already occur at depths ≥100 cm. The vertical percolation fluxes were reduced by the RWU throughout the soil profile. The groundwater recharge varied temporally due to combination of rainfall, RWU, and evapotranspiration, resulting in annual rates ranging from 60 to 470 mm yr^{-1} at S1, corresponding to 5 and 29% of rainfall, respectively. These results were lower than the recharge rates at S2, which ranged from 230 to 620 mm yr^{-1}, corresponding to 18 and 38% of rainfall, respectively. Given the results of the previous sections, the most important factors distinguishing the recharge rates

at S1 (upstream area) and S2 (downstream area) are the soil hydraulic properties and groundwater table depths.
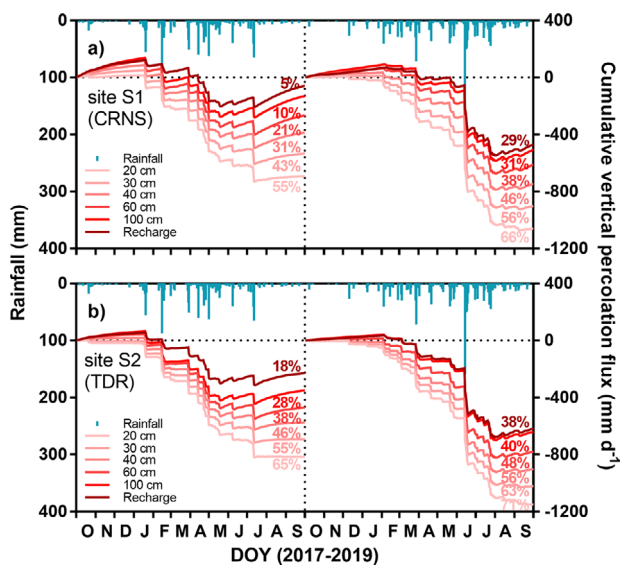
The cumulative groundwater recharge flux was compared with the WTF estimates at S1 and S2 for S_y equal to 0.10, 0.16, and 0.24 (Figure 11). The specific yield of 0.16 found at S1 was similar to the mean estimate of ~0.15 found in a management zone of water resources close to GEB (Braga et al., 2015), which acted as a reference value, whereas 0.10 and 0.24 are an estimated minimum and maximum limit, respectively. The simulations at S1 showed good performance in both hydrological years for S_y equal to 0.16, underlined by KGE equal to 0.83 and 0.79. However, using the same S_y value, estimations at S2 in the rainy hydrological year resulted in a lower accuracy, indicated by a KGE equal to just 0.36. On the other hand, the KGE was 0.84 when using S_y equal to 0.24. This behavior can be explained in part by the sensitivity of S_y values according to the depth to the groundwater table (Dettmann & Bechtold, 2016), as well as by the TDR-based point-scale calibration of soil hydraulic parameters used for the GWR estimation. The better match between the simulated recharge at S1 to the WTF estimates can be explained by the integrative nature and wider spatial range of influencing moisture as association of both data products, the neutron count rate being representative of the field-scale soil moisture and the groundwater table fluctuations also representing the area average behavior. Although the study period comprises two contrasting hydrological years, it needs to be emphasized that limitations to the implications may arise from the short timeframe. Strong seasonality and extreme hydrological conditions, which could be expected in this climate, were not sufficiently represented by this study (Wendland et al., 2007). Nevertheless, the basic conclusion is that using CRNS data compared with point-scale soil moisture data to inversely estimate soil hydraulic parameters to derive dynamic groundwater recharge rates at field scale is at least a suitable, probably more representative alternative.
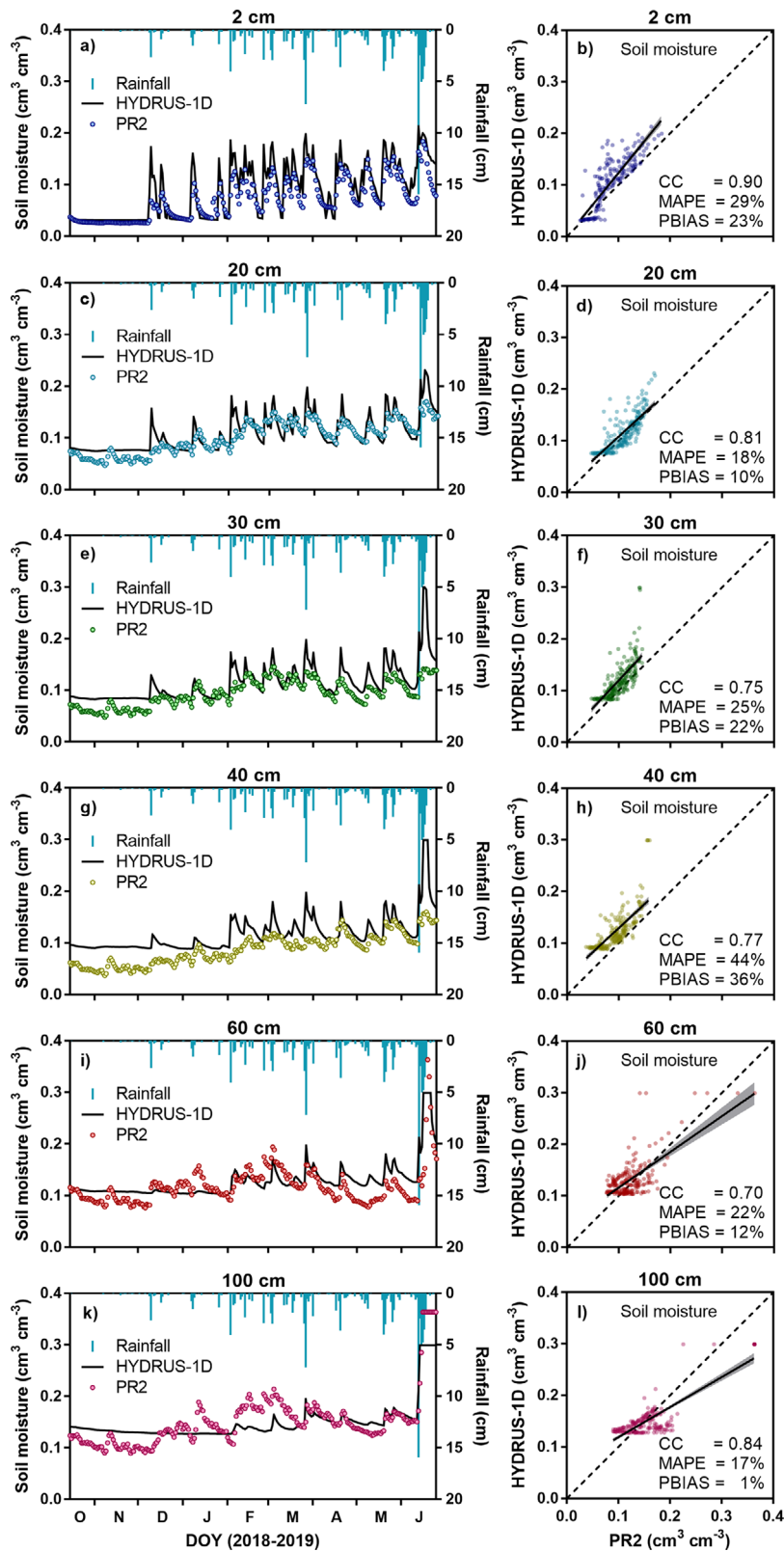
FIGURE 8 Soil moisture simulation at S1, based on soil hydraulic properties calibrated with cosmic-ray neutron sensing (CRNS) data plotted for validation against the PR2 data in the depths of (a, b) 2 cm, (c, d) 20 cm, (e, f) 30 cm, (g, h) 40 cm, (i, j) 60 cm, and (k, l) 100 cm (only one probe delivered consistent data for the full measurement period). CC, correlation coefficient; MAPE, mean absolute percentage error; PBIAS, percentage bias
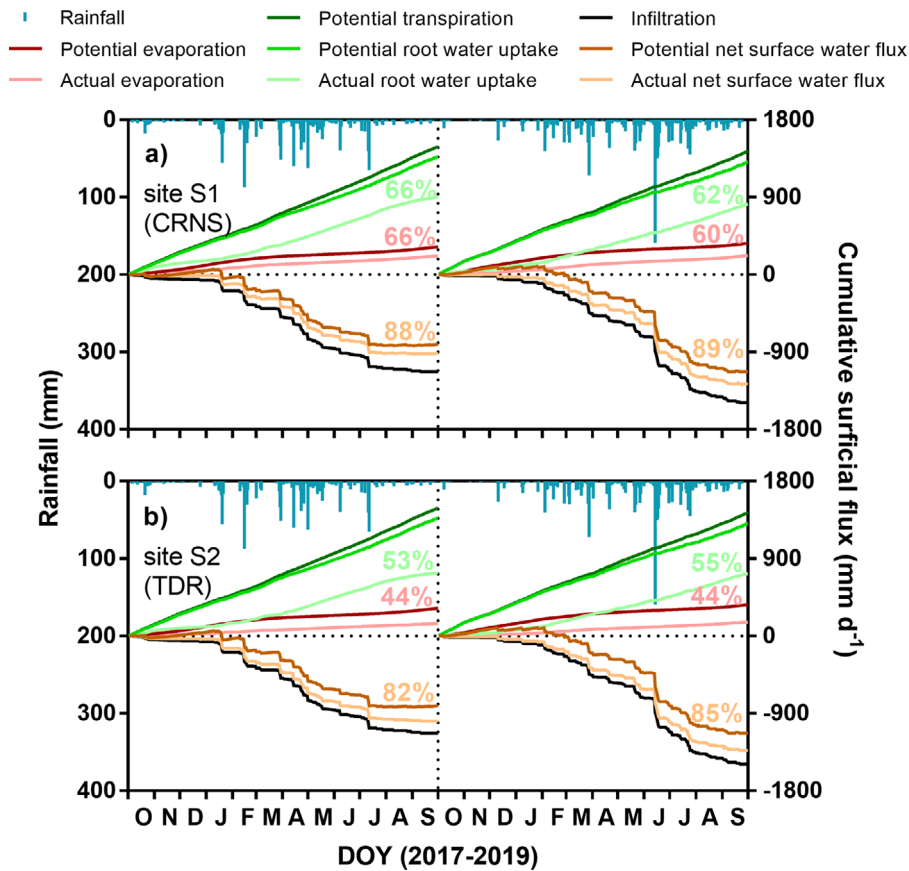
FIGURE 9 Cumulative water flux of evaporation, transpiration, root water uptake, infiltration, and net surface water flux at (a) S1 and (b) S2. Showing similar ratios of potential to actual net surface fluxes (infiltration minus evaporation) for both sites but distinct evapotranspiration rates. Especially the ratio of potential to actual evaporation is low at S2 (~44%) compared with S1 (~63%). CRNS, cosmic-ray neutron sensing; TDR, time-domain reflectometry; DOY, day of year


FIGURE 10 Cumulative vertical percolation flux at (a) S1 and (b) S2, in the depths of 20, 30, 40, 60, and 100 cm, and the variable bottom boundary for the dynamic groundwater recharge rate estimation. CRNS, cosmic-ray neutron sensing; TDR, time-domain reflectometry; DOY, day of year

4 | CONCLUSION

The study assessed the capacity of CRNS for (a) monitoring soil moisture at the intermediate scale under the unfavorable, humid tropic conditions, and in (b) the use of CRNS to inversely calibrate soil hydraulic parameters and simulate dynamic groundwater recharge rates. The study used CRNS data from two contrasting hydrological years in an experimental basin and supported by a range of ground truth information. The results showed that the CRNS-based soil moisture time series responded consistently in alignment with the observed soil moisture profile measurements, despite its relatively scattered dataset resulting from the low incoming neutron count rate.

Using the COSMIC operator coupled with HYDRUS-1D model enabled to inversely calibrate the soil hydraulic parameters based on CRNS data, and, in turn, to satisfactorily simulate the aboveground neutron count rate and soil moisture time series. The resulting soil hydraulic parameters were found to be in line with ranges reported in literature, whereas the saturated hydraulic conductivity was successfully validated
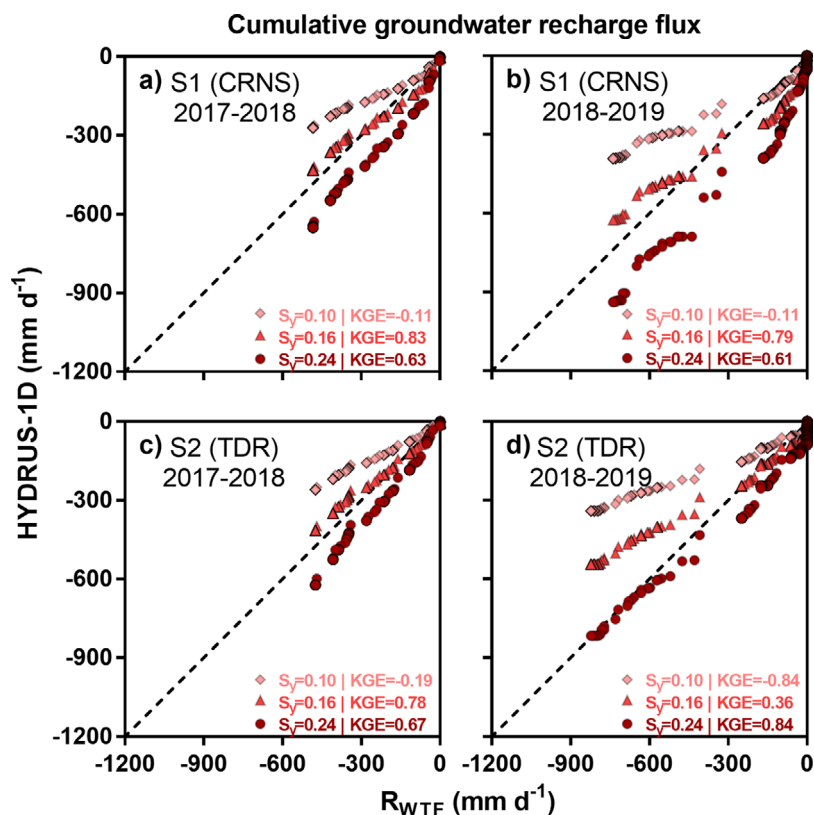
FIGURE 11 Comparison of the cumulative groundwater recharge flux estimated by the one-dimensional soil hydrological model HYDRUS-1D and water table fluctuation method for specific yield (S_y) equal to 0.10, 0.16, and 0.24, at (a, b) S1 and (c, d) S2. The negative sign for the flux indicates the downward direction. CRNS, cosmic-ray neutron sensing; TDR, time-domain reflectometry; KGE, Kling–Gupta efficiency; R_{WTF}, groundwater recharge estimated using the water table fluctuation method

by local experiments. Moreover, the HYDRUS-1D model enabled us to simulate the vertical water percolation fluxes of the root zone and the dynamic groundwater recharge rates at the variable bottom boundary. Compared with WTF-based groundwater recharge estimates, the CRNS-based simulated recharge performed better than simulated recharge rates based on point-scale data (used to optimize the soil hydraulic properties). Given the results presented here, we concluded that CRNS derived hydrological parameters could provide a more effective support to derive field-scale groundwater recharge rates, as it represents integral information over an intermediate scale, even under tropical conditions.

Recent developments in CRNS detectors towards different designs and more sensitive devices (Stevanato et al., 2019; Weimar et al., 2020) could help to address unfavorable conditions with respect to low neutron count rates and might provide even more precise results in the future. This encourages the adoption of such technology in developing tropical countries, whose forest protection and aquifer groundwater level conservation are essential for preserving the terrestrial and estuarine biodiversity, as well as whose economy strongly depends on agricultural practices. Accordingly, it is expected that these findings will increasingly promote the CRNS hydrological applications to provide appropriate estimates of groundwater recharge rates, important for diligent and sustainable management of groundwater resources by decision-makers in regions with similar characteristics. However, further studies exploring the hydrological poten-

tials of the CRNS-based simulations, related to dynamic groundwater recharge rates in other tropical wet and semiarid regions, are strongly recommended to expand the knowledge of water resources and to foster the good sustainable practices.

Oliveira Galvão, which undoubtedly contributed to improve the quality of the paper.

CONFLICT OF INTEREST
The authors declare that they have no known competing financial interests or personal relationships that could have appeared to influence the work reported in this paper.

ORCID
Luís Romero Barbosa https://orcid.org/0000-0002-1104-2623

Victor Hugo R. Coelho https://orcid.org/0000-0002-6669-4856

Lena M. Scheiffele https://orcid.org/0000-0003-3621-680X

Gabriele Baroni https://orcid.org/0000-0003-2873-7162

Geraldo M. Ramos Filho https://orcid.org/0000-0002-7819-2511

Suzana M. G. L. Montenegro https://orcid.org/0000-0002-2520-5761

Cristiano das N. Almeida https://orcid.org/0000-0002-3655-5396

Sascha E. Oswald https://orcid.org/0000-0003-1667-0060

REFERENCES
Alvares, C. A., Stape, J. L., Sentelhas, P. C., De Moraes Gonçalves, J. L., & Sparovek, G. (2013). Köppen's climate classification map for Brazil. *Meteorologische Zeitschrift*, *22*, 711–728. https://doi.org/10.1127/0941-2948/2013/0507

Andreasen, M., Jensen, K. H., Desilets, D., Franz, T. E., Zreda, M., Bogena, H. R., & Looms, M. C. (2017). Status and perspectives on the cosmic-ray neutron method for soil moisture estimation and other environmental science applications. *Vadose Zone Journal*, *16*(8). https://doi.org/10.2136/vzj2017.04.0086

Baatz, R., Bogena, H. R., Hendricks Franssen, H. - J., Huisman, J. A., Montzka, C., & Vereecken, H. (2015). An empirical vegetation correction for soil water content quantification using cosmic ray probes. *Water Resources Research*, *51*, 2030–2046. https://doi.org/10.1002/2014WR016443

Baatz, R., Bogena, H. R., Hendricks Franssen, H.-J., Huisman, J. A., Qu, W., Montzka, C., & Vereecken, H. (2014). Calibration of a catchment scale cosmic-ray probe network: A comparison of three parameterization methods. *Journal of Hydrology*, *516*, 231–244. https://doi.org/10.1016/j.jhydrol.2014.02.026

Baatz, R., Hendricks Franssen, H.-J., Han, X., Hoar, T., Bogena, H. R., & Vereecken, H. (2017). Evaluation of a cosmic-ray neutron sensor network for improved land surface model prediction. *Hydrology and Earth System Sciences*, *21*, 2509–2530. https://doi.org/10.5194/hess-21-2509-2017

Barbosa, L. R. (2020). *Groundwater recharge in tropical wet regions via GIS-based methods and cosmic-ray neutron sensing*. (Doctoral dissertation, Universität Potsdam). https://doi.org/10.25932/publishup-46064

Barbosa, L. R., Lira, N. B. D., Coelho, V. H. R., Silans, A. M. B. P. D.e, Gadêlha, A. N., & Almeida, C. D. N. (2019). Stability of soil moisture patterns retrieved at different temporal resolutions in a tropical watershed. *Revista Brasileira de Ciência do Solo*, *43*, 1–21. https://doi.org/10.1590/18069657rbcs20180236

Baroni, G., & Oswald, S. E. (2015). A scaling approach for the assessment of biomass changes and rainfall interception using cosmic-ray neutron sensing. *Journal of Hydrology*, *525*, 264–276. https://doi.org/10.1016/j.jhydrol.2015.03.053

Baroni, G., Oswald, S. E., & Rivera Villarreyes, C. A. (2012). A global uncertainty and sensitivity procedure for the assessment of groundwater recharge distribution via hydrological models. In K. Rink, T. Fischer, A. Gräbe, & O. Kolditz (Eds.), *Models—Repositories of knowledge: Proceedings of ModelCARE201* (Publ. 355, pp. 71–77). International Association of Hydrological Sciences. http://hydrologie.org/redbooks/a355/iahs_355_0071.pdf

Baroni, G., Scheiffele, L. M., Schrön, M., Ingwersen, J., & Oswald, S. E. (2018). Uncertainty, sensitivity and improvements in soil moisture estimation with cosmic-ray neutron sensing. *Journal of Hydrology*, *564*, 873–887. https://doi.org/10.1016/j.jhydrol.2018.07.053

Bastiaanssen, W. G. M., Pelgrum, H., Wang, J., Ma, Y., Moreno, J. F., Roerink, G. J., & van Der Wal, T. (1998). A remote sensing surface energy balance algorithm for land (SEBAL), Part 1: Formulation. *Journal of Hydrology*, *212–213*, 213–229. https://doi.org/10.1016/S0022-1694(98)00254-6

Batalha, M. S., Barbosa, M. C., Faybishenko, B., & van Genuchten, M. Th. (2018). Effect of temporal averaging of meteorological data on predictions of groundwater recharge. *Journal of Hydrology and Hydromechanics*, *66*, 143–152. https://doi.org/10.1515/johh-2017-0051

Blonquist, J. M., Jones, S. B., & Robinson, D. A. (2005). Standardizing characterization of electromagnetic water content sensors: Part 2. Evaluation of seven sensing systems. *Vadose Zone Journal*, *4*, 1059–1069. https://doi.org/10.2136/vzj2004.0141

Bogena, H. R., Herbst, M., Huisman, J. A., Rosenbaum, U., Weuthen, A., & Vereecken, H. (2010). Potential of wireless sensor networks for measuring soil water content variability. *Vadose Zone Journal*, *9*, 1002–1013. https://doi.org/10.2136/vzj2009.0173

Bogena, H. R., Huisman, J. A., Baatz, R., Hendricks Franssen, H.-J., & Vereecken, H. (2013). Accuracy of the cosmic-ray soil water content probe in humid forest ecosystems: The worst case scenario. *Water Resources Research*, *49*, 5778–5791. https://doi.org/10.1002/wrcr.20463

Bogena, H. R., Huisman, J. A., Güntner, A., Hübner, C., Kusche, J., Jonard, F., Vey, S., & Vereecken, H. (2015). Emerging methods for noninvasive sensing of soil moisture dynamics from field to catchment scale: A review. *WIREs Water*, 2, 635–647. https://doi.org/10.1002/wat2.1097

Bouwer, H., & Rice, R. C. (1976). A slug test for determining hydraulic conductivity of unconfined aquifers with completely or partially penetrating wells. *Water Resources Research*, 12, 423–428. https://doi.org/10.1029/WR012i003p00423

Braga, A., Rêgo, J., & Galvão, C. (2015). Variação intra-sazonal da potencialidade hídrica subterrânea e sua influência na outorga. *Revista Brasileira de Recursos Hídricos*, 20, 647–656. https://doi.org/10.21168/rbrh.v20n3.p647-656

Brunetti, G., Šimůnek, J., Bogena, H., Baatz, R., Huisman, J. A., Dahlke, H., & Vereecken, H. (2019). On the information content of cosmic-ray neutron data in the inverse estimation of soil hydraulic properties. *Vadose Zone Journal*, 18, 1–24. https://doi.org/10.2136/vzj2018.06.0123

Brunner, P., Bauer, P., Eugster, M., & Kinzelbach, W. (2004). Using remote sensing to regionalize local precipitation recharge rates obtained from the chloride method. *Journal of Hydrology*, 294, 241–250. https://doi.org/10.1016/j.jhydrol.2004.02.023

Cai, Z., & Ofterdinger, U. (2016). Analysis of groundwater-level response to rainfall and estimation of annual recharge in fractured hard rock aquifers, NW Ireland. *Journal of Hydrology*, 535, 71–84. https://doi.org/10.1016/j.jhydrol.2016.01.066

Callahan, T. J., Vulava, V. M., Passarello, M. C., & Garrett, C. G. (2012). Estimating groundwater recharge in lowland watersheds. *Hydrological Processes*, 26, 2845–2855. https://doi.org/10.1002/hyp.8356

Chen, M., Willgoose, G. R., & Saco, P. M. (2014). Spatial prediction of temporal soil moisture dynamics using HYDRUS-1D. *Hydrological Processes*, 28, 171–185. https://doi.org/10.1002/hyp.9518

Cooper, M., Boschi, R. S., Silva, L. F. S. D. A, Toma, R. S., & Vidal-Torrado, P. (2017). Hydro-physical characterization of soils under the Restinga Forest. *Scientia Agricola*, 74, 393–400. https://doi.org/10.1590/1678-992x-2016-0103

Cristiano, P. M., Campanello, P. I., Bucci, S. J., Rodriguez, S. A., Lezcano, O. A., Scholz, F. G., Madanes, N., Di Francescantonio, D., Carrasco, L. O., Zhang, Y. -. J., & Goldstein, G. (2015). Evapotranspiration of subtropical forests and tree plantations: A comparative analysis at different temporal and spatial scales. *Agricultural and Forest Meteorology*, 203, 96–106. https://doi.org/10.1016/j.agrformet.2015.01.007

de Oliveira, G., Moraes, E. C., Brunsell, N. A., Shimabukuro, Y. E., Mataveli, G. A. V., & dos Santos, T. V. (2016). Analysis of precipitation and evapotranspiration in Atlantic Rainforest remnants in Southeastern Brazil from remote sensing data. In J. Blanco (Ed.), *Tropical forests: The challenges of maintaining ecosystem services while managing the landscape* (pp. 93–112). InTech. https://doi.org/10.5772/64533

Delin, G. N., Healy, R. W., Lorenz, D. L., & Nimmo, J. R. (2007). Comparison of local- to regional-scale estimates of ground-water recharge in Minnesota, USA. *Journal of Hydrology*, 334, 231–249. https://doi.org/10.1016/j.jhydrol.2006.10.010

Delta-T. (2016). *User manual for the Profile Probe* (Type PR2). Delta-T Devices. http://www.delta-t.co.uk/wp-content/uploads/2017/02/PR2_user_manual_version_5.0.pdf

Desilets, D., & Zreda, M. (2001). On scaling cosmogenic nuclide production rates for altitude and latitude using cosmic-ray measurements. *Earth and Planetary Science Letters*, 193, 213–225. https://doi.org/10.1016/S0012-821X(01)00477-0

Desilets, D., Zreda, M., & Ferré, T. P. A. (2010). Nature's neutron probe: Land surface hydrology at an elusive scale with cosmic rays. *Water Resources Research*, 46(11). https://doi.org/10.1029/2009WR008726

Desilets, D., Zreda, M., & Prabu, T. (2006). Extended scaling factors for in situ cosmogenic nuclides: New measurements at low latitude. *Earth and Planetary Science Letters*, 246, 265–276. https://doi.org/10.1016/j.epsl.2006.03.051

Dettmann, U., & Bechtold, M. (2016). One-dimensional expression to calculate specific yield for shallow groundwater systems with microrelief. *Hydrological Processes*, 30, 334–340. https://doi.org/10.1002/hyp.10637

Dimitrova-Petrova, K., Geris, J., Wilkinson, M. E., Rosolem, R., Verrot, L., Lilly, A., & Soulsby, C. (2020). Opportunities and challenges in using catchment-scale storage estimates from cosmic ray neutron sensors for rainfall-runoff modelling. *Journal of Hydrology*, 586, 124878. https://doi.org/10.1016/j.jhydrol.2020.124878

Duygu, M. B., & Akyürek, Z. (2019). Using cosmic-ray neutron probes in validating satellite soil moisture products and land surface models. *Water*, 11, 1362. https://doi.org/10.3390/w11071362

Evans, J. G., Ward, H. C., Blake, J. R., Hewitt, E. J., Morrison, R., Fry, M., Ball, L. A., Doughty, L. C., Libre, J. W., Hitt, O. E., Rylett, D., Ellis, R. J., Warwick, A. C., Brooks, M., Parkes, M. A., Wright, G. M. H., Singer, A. C., Boorman, D. B., & Jenkins, A. (2016). Soil water content in southern England derived from a cosmic-ray soil moisture observing system: COSMOS-UK. *Hydrological Processes*, 30, 4987–4999. https://doi.org/10.1002/hyp.10929

Famiglietti, J. S., Cazenave, A., Eicker, A., Reager, J. T., Rodell, M., & Velicogna, I. (2015). Satellites provide the big picture. *Science*, 349, 684–685. https://doi.org/10.1126/science.aac9238

Feddes, R. A., Kowalik, P. J., & Zaradny, H. (1978). *Simulation of field water use and crop yield*. John Wiley & Sons. http://edepot.wur.nl/172222

Fersch, B., Francke, T., Heistermann, M., Schrön, M., Döpper, V., Jakobi, J., Baroni, G., Blume, T., Bogena, H., Budach, C., Gränzig, T., Förster, M., Güntner, A., Hendricks Franssen, H.-J., Kasner, M., Köhli, M., Kleinschmit, B., Kunstmann, H., Patil, A., … Oswald, S. (2020). A dense network of cosmic-ray neutron sensors for soil moisture observation in a highly instrumented pre-Alpine headwater catchment in Germany. *Earth System Science Data*, 12, 2289–2309. https://doi.org/10.5194/essd-12-2289-2020

Finkenbiner, C. E., Franz, T. E., Gibson, J., Heeren, D. M., & Luck, J. (2018). Integration of hydrogeophysical datasets and empirical orthogonal functions for improved irrigation water management. *Precision Agriculture*, 20, 78–100. https://doi.org/10.1007/s11119-018-9582-5

Franz, T. E., Wahbi, A., Zhang, J., Vreugdenhil, M., Heng, L., Dercon, G., Strauss, P., Brocca, L., & Wagner, W. (2020). Practical data products from cosmic-ray neutron sensing for hydrological applications. *Frontiers in Water*, 2, 9. https://doi.org/10.3389/frwa.2020.00009

Franz, T. E., Zreda, M., Ferre, T. P. A., & Rosolem, R. (2013). An assessment of the effect of horizontal soil moisture heterogeneity on the area-average measurement of cosmic-ray neutrons. *Water Resources Research*, 49, 6450–6458. https://doi.org/10.1002/wrcr.20530

Franz, T. E., Zreda, M., Rosolem, R., Hornbuckle, B. K., Irvin, S. L., Adams, H., Kolb, T. E., Zweck, C., & Shuttleworth, W. J. (2013). Ecosystem-scale measurements of biomass water using cosmic ray

neutrons. *Geophysical Research Letters*, *40*, 3929–3933. https://doi.org/10.1002/grl.50791

Gibson, J., & Franz, T. E. (2018). Spatial prediction of near surface soil water retention functions using hydrogeophysics and empirical orthogonal functions. *Journal of Hydrology*, *561*, 372–383. https://doi.org/10.1016/j.jhydrol.2018.03.046

Gleeson, T., Wada, Y., Bierkens, M. F. P., & van Beek, L. P. H. (2012). Water balance of global aquifers revealed by groundwater footprint. *Nature*, *488*, 197–200. https://doi.org/10.1038/nature11295

Graeff, T., Zehe, E., Schlaeger, S., Morgner, M., Bauer, A., Becker, R., Creutzfeldt, B., & Bronstert, A. (2010). A quality assessment of spatial TDR soil moisture measurements in homogenous and heterogeneous media with laboratory experiments. *Hydrology and Earth System Sciences*, *14*, 1007–1020. https://doi.org/10.5194/hess-14-1007-2010

Graham, S. L., Srinivasan, M. S., Faulkner, N., & Carrick, S. (2018). Soil hydraulic modeling outcomes with four parameterization methods: Comparing soil description and inverse estimation approaches. *Vadose Zone Journal*, *17*, 170002. https://doi.org/10.2136/vzj2017.01.0002

Han, M., Zhao, C., Šimůnek, J., & Feng, G. (2015). Evaluating the impact of groundwater on cotton growth and root zone water balance using HYDRUS-1D coupled with a crop growth model. *Agricultural Water Management*, *160*, 64–75. https://doi.org/10.1016/j.agwat.2015.06.028

Hawdon, A., Mcjannet, D., & Wallace, J. (2014). Calibration and correction procedures for cosmic-ray neutron soil moisture probes located across Australia. *Water Resources Research*, *50*, 5029–5043. https://doi.org/10.1002/2013WR015138

Heidbüchel, I., Güntner, A., & Blume, T. (2016). Use of cosmic-ray neutron sensors for soil moisture monitoring in forests. *Hydrology and Earth System Sciences*, *20*, 1269–1288. https://doi.org/10.5194/hess-20-1269-2016

Heistermann, M., Francke, T., Schrön, M., & Oswald, S. E. (2021). Spatio-temporal soil moisture retrieval at the catchment-scale using a dense network of cosmic-ray neutron sensors. *Hydrology and Earth System Sciences*. https://doi.org/10.5194/hess-2021-25

Hendrick, L. D., & Edge, R. D. (1966). Cosmic-ray neutrons near the Earth. *Physical Review*, *145*, 1023–1025. https://doi.org/10.1103/PhysRev.145.1023

Hoffman, G. J., & van Genuchten, M. Th. (1983). Soil properties and efficient water use: Water management for salinity control. In H. M. Taylor, W. R. Jordan, & T. R. Sinclair (Eds.), *Limitations and efficient water use in crop production* (pp. 73–85). ASA and CSSA. https://doi.org/10.2134/1983.limitationstoefficientwateruse.c5

Hornero, J., Manzano, M., Ortega, L., & Custodio, E. (2016). Integrating soil water and tracer balances, numerical modelling and GIS tools to estimate regional groundwater recharge: Application to the Alcadozo Aquifer System (SE Spain). *Science of the Total Environment*, *568*, 415–432. https://doi.org/10.1016/j.scitotenv.2016.06.011

Huete, A. R. (1988). A soil-adjusted vegetation index (SAVI). *Remote Sensing of Environment*, *25*, 295–209. https://doi.org/10.1016/0034-4257(88)90106-X

Ishida, D. A., Montes, C. R., Lucas, Y., Pereira, O. J. R., Merdy, P., & Melfi, A. J. (2014). Genetic relationships between ferralsols, podzols and white kaolin in Amazonia. *European Journal of Scientific Research*, *65*, 706–717. https://doi.org/10.1111/ejss.12167

IUSS Working Group WRB. (2015). *World Reference Base for Soil Resources 2014: International soil classification system for naming soils and creating legends for soil maps. Update 2015* (World Soil Resour. Rep. 106). FAO. http://www.fao.org/3/a-i3794en.pdf

Iwema, J., Rosolem, R., Baatz, R., Wagener, T., & Bogena, H. R. (2015). Investigating temporal field sampling strategies for site-specific calibration of three soil moisture–neutron intensity parameterisation methods. *Hydrology and Earth System Sciences*, *19*, 3203–3216. https://doi.org/10.5194/hess-19-3203-2015

Jakobi, J., Huisman, J. A., Vereecken, H., Diekkrüger, B., & Bogena, H. R. (2018). Cosmic ray neutron sensing for simultaneous soil water content and biomass quantification in drought conditions. *Water Resources Research*, *54*, 7383–7402. https://doi.org/10.1029/2018WR022692

Jankowski, M. (2014). The evidence of lateral podzolization in sandy soils of northern Poland. *Catena*, *112*, 139–147. https://doi.org/10.1016/j.catena.2013.03.013

Jasechko, S., Birks, S. J., Gleeson, T., Wada, Y., Fawcett, P. J., Sharp, Z. D., Mcdonnell, J. J., & Welker, J. M. (2014). The pronounced seasonality of global groundwater recharge. *Water Resources Research*, *50*, 1–23. https://doi.org/10.1002/2014WR015809

Jie, Z., Van Heyden, J., Bendel, D., & Barthel, R. (2011). Combination of soil-water balance models and water-table fluctuation methods for evaluation and improvement of groundwater recharge calculations. *Hydrogeology Journal*, *19*, 1487–1502. https://doi.org/10.1007/s10040-011-0772-8

Köhli, M., Schrön, M., Zreda, M., Schmidt, U., Dietrich, P., & Zacharias, S. (2015). Footprint characteristics revised for field-scale soil moisture monitoring with cosmic-ray neutrons. *Water Resources Research*, *51*, 5772–5790. https://doi.org/10.1002/2015WR017169

Köhli, M., Weimar, J., Schrön, M., Baatz, R., & Schmidt, U. (2021). Soil moisture and air humidity dependence of the above-ground cosmic-ray neutron intensity. *Frontiers in Water*, *2*, 544847. https://doi.org/10.3389/frwa.2020.544847

Li, D., Schrön, M., Köhli, M., Bogena, H., Weimar, J., Jiménez Bello, M. A., Han, X., Martínez Gimeno, M. A., Zacharias, S., Vereecken, H., & Hendricks Franssen, H.-J. (2019). Can drip irrigation be scheduled with cosmic-ray neutron sensing? *Vadose Zone Journal*, *18*, 190053. https://doi.org/10.2136/vzj2019.05.0053

Lv, L., Franz, T. E., Robinson, D. A., & Jones, S. B. (2014). Measured and modeled soil moisture compared with cosmic-ray neutron probe estimates in a mixed forest. *Vadose Zone Journal*, *13*(12). https://doi.org/10.2136/vzj2014.06.0077

Mathias, S. A., Sorensen, J. P. R., & Butler, A. P. (2017). Soil moisture data as a constraint for groundwater recharge estimation. *Journal of Hydrology*, *552*, 258–266. https://doi.org/10.1016/j.jhydrol.2017.06.040

Melo, D. D. E. C. D., Wendland, E., & Guanabara, R. C. (2015). Estimate of groundwater recharge based on water balance in the unsaturated soil zone. *Revista Brasileira de Ciência do Solo*, *39*, 1335–1343. https://doi.org/10.1590/01000683rbcs20140740

Moeck, C., Grech-Cumbo, N., Podgorski, J., Bretzler, A., Gurdak, J. J., Berg, M., & Schirmer, M. (2020). A global-scale dataset of direct natural groundwater recharge rates: A review of variables, processes and relationships. *Science of the Total Environment*, *717*, 137042. https://doi.org/10.1016/j.scitotenv.2020.137042

Mohan, C., Western, A. W., Wei, Y., & Saft, M. (2018). Predicting groundwater recharge for varying land cover and climate conditions: A global meta-study. *Hydrology and Earth System Sciences*, *22*, 2689–2703. https://doi.org/10.5194/hess-22-2689-2018

Montzka, C., Bogena, H., Zreda, M., Monerris, A., Morrison, R., Muddu, S., & Vereecken, H. (2017). Validation of spaceborne and modelled surface soil moisture products with cosmic-ray neutron probes. *Remote Sensing*, *9*(2). https://doi.org/10.3390/rs9020103

Mualem, Y. (1976). A new model for predicting the hydraulic conductivity of unsaturated porous media. *Water Resources Research*, *12*, 513–522. https://doi.org/10.1029/WR012i003p00513

Neuman, S. P., Feddes, R. A., & Bresler, E. (1974). *Finite element simulation of flow in saturated-unsaturated soils considering water uptake by plants* (Third Annual Report, Project A10- SWC-77). FAO. http://agris.fao.org/agris-search/search.do?recordID=US201300536275

Nimmo, J. R., Horowitz, C., & Mitchell, L. (2015). Discrete-storm water-table fluctuation method to estimate episodic recharge. *Groundwater*, *53*, 282–292. https://doi.org/10.1111/gwat.12177

Penman, H. L. (1948). Natural evaporation from open water, bare soil and grass. *Proceedings of the Royal Society of London*, *193*, 120–145. https://doi.org/10.1098/rspa.1948.0037

PERH-PB. (2006). *Paraíba State Water Resources Master Plan. Item 5.1: Potencialidade, disponibilidade e capacidade de armazenamento potencial*. Governo do Estado da Paraíba. http://www.aesa.pb.gov.br/aesa-website/wp-content/uploads/2016/11/PE_22.pdf

Pinheiro, E. A. R., Costa, C. A. G., & De Araújo, J. C. (2013). Effective root depth of the Caatinga biome. *Journal of Arid Environments*, *89*, 1–4. https://doi.org/10.1016/j.jaridenv.2012.10.003

Raoufi, R., & Beighley, E. (2017). Estimating daily global evapotranspiration using Penman–Monteith equation and remotely sensed land surface temperature. *Remote Sensing*, *9*, 1138. https://doi.org/10.3390/rs9111138

Ries, F., Lange, J., Schmidt, S., Puhlmann, H., & Sauter, M. (2015). Recharge estimation and soil moisture dynamics in a Mediterranean, semi-arid karst region. *Hydrology and Earth System Sciences*, *19*, 1439–1456. https://doi.org/10.5194/hess-19-1439-2015

Rivera Villarreyes, C. A., Baroni, G., & Oswald, S. E. (2011). Integral quantification of seasonal soil moisture changes in farmland by cosmic-ray neutrons. *Hydrology and Earth System Sciences*, *15*, 3843–3859. https://doi.org/10.5194/hess-15-3843-2011

Rivera Villarreyes, C. A., Baroni, G., & Oswald, S. E. (2014). Inverse modelling of cosmic-ray soil moisture for field-scale soil hydraulic parameters. *European Journal of Soil Science*, *65*, 876–886. https://doi.org/10.1111/ejss.12162

Robinson, D. A., Campbell, C. S., Hopmans, J. W., Hornbuckle, B. K., Jones, S. B., Knight, R., Ogden, F., Selker, J., & Wendroth, O. (2008). Soil moisture measurement for ecological and hydrological watershed-scale observatories: A review. *Vadose Zone Journal*, *7*, 358–389. https://doi.org/10.2136/vzj2007.0143

Rosolem, R., Hoar, T., Arellano, A., Anderson, J. L., Shuttleworth, W. J., Zeng, X., & Franz, T. E. (2014). Translating aboveground cosmic-ray neutron intensity to high-frequency soil moisture profiles at sub-kilometer scale. *Hydrology and Earth System Sciences*, *18*, 4363–4379. https://doi.org/10.5194/hess-18-4363-2014

Rosolem, R., Shuttleworth, W. J., Zreda, M., Franz, T. E., Zeng, X., & Kurc, S. A. (2013). The effect of atmospheric water vapor on neutron count in the cosmic-ray soil moisture observing system. *Journal of Hydrometeorology*, *14*, 1659–1672. https://doi.org/10.1175/JHM-D-12-0120.1

Rossetti, D. F., Góes, A. M., Bezerra, F. H. R., Valeriano, M. M., Brito-Neves, B. B., & Ochoa, F. L. (2012). Contribution to the stratigraphy of the Onshore Paraíba basin, Brazil. *Anais da Academia Brasileira de Ciências*, *84*, 313–333. https://doi.org/10.1590/S0001-37652012005000026

Sadeghi, M., Tuller, M., Warrick, A. W., Babaeian, E., Parajuli, K., Gohardoust, M. R., & Jones, S. B. (2018). An analytical model for estimation of land surface net water flux from near-surface soil moisture observations. *Journal of Hydrology*, *570*, 26–37. https://doi.org/10.1016/j.jhydrol.2018.12.038

Sales, E. G., das N Almeida, C., Farias, A. S., & Coelho, V. H. R. (2014). Hydrodynamic characterization of soils within a representative watershed in northeast Brazil. *Proceedings of the International Association of Hydrological Sciences*, *364*, 94–99. https://doi.org/10.5194/piahs-364-94-2014

Santos, C., Silva, J., & Silva, R. (2012). Caracterização Hidrodinâmica dos Solos da Bacia Experimental do Riacho Guaraíra Utilizando o Método Beerkan. *Revista Brasileira de Recursos Hídricos*, *17*, 149–160. https://doi.org/10.21168/rbrh.v17n4.p149-160

Schaap, M. G., Leij, F. J., & van Genuchten, M. Th. (2001). ROSETTA: A computer program for estimating soil hydraulic parameters with hierarchical pedotransfer functions. *Journal of Hydrology*, *251*, 163–176. https://doi.org/10.1016/S0022-1694(01)00466-8

Schattan, P., Baroni, G., Oswald, S. E., Schöber, J., Fey, C., Kormann, C., Huttenlau, M., & Achleitner, S. (2017). Continuous monitoring of snowpack dynamics in alpine terrain by aboveground neutron sensing. *Water Resources Research*, *53*, 3615–3634. https://doi.org/10.1002/2016WR020234

Scheiffele, L. M., Baroni, G., Franz, T. E., Jakobi, J., & Oswald, S. E. (2020). A profile shape correction to reduce the vertical sensitivity of cosmic-ray neutron sensing of soil moisture. *Vadose Zone Journal.*, *19*, e20083. https://doi.org/10.1002/vzj2.20083

Schrön, M., Köhli, M., Scheiffele, L., Iwema, J., Bogena, H. R., Lv, L., Martini, E., Baroni, G., Rosolem, R., Weimar, J., Mai, J., Cuntz, M., Rebmann, C., Oswald, S. E., Dietrich, P., Schmidt, U., & Zacharias, S. (2017). Improving calibration and validation of cosmic-ray neutron sensors in the light of spatial sensitivity. *Hydrology and Earth System Sciences*, *21*, 5009–5030. https://doi.org/10.5194/hess-21-5009-2017

Schrön, M., Rosolem, R., Köhli, M., Piussi, L., Schröter, I., Iwema, J., Kögler, S., Oswald, S. E., Wollschläger, U., Samaniego, L., Dietrich, P., & Zacharias, S. (2018). Cosmic-ray neutron rover surveys of field soil moisture and the influence of roads. *Water Resources Research*, *54*, 6441–6459. https://doi.org/10.1029/2017WR021719

Schrön, M., Zacharias, S., Womack, G., Köhli, M., Desilets, D., Oswald, S. E., Bumberger, J., Mollenhauer, H., Kögler, S., Remmler, P., Kasner, M., Denk, A., & Dietrich, P. (2018). Intercomparison of cosmic-ray neutron sensors and water balance monitoring in an urban environment. *Geoscientific Instrumentation Methods and Data Systems*, *7*, 83–99. https://doi.org/10.5194/gi-7-83-2018

Shuttleworth, W. J. (1993). Evaporation. In D. R. Maidment (Ed.), *Handbook of hydrology* (pp. 4.1–4.53). McGraw Hill. http://pdfs.semanticscholar.org/8dad/8b5a1ff7c629980b8ffedcc1db9bbc69f61e.pdf

Shuttleworth, J., Rosolem, R., Zreda, M., & Franz, T. (2013). The COsmic-ray Soil Moisture Interaction Code (COSMIC) for use in data assimilation. *Hydrology and Earth System Sciences*, *17*, 3205–3217. https://doi.org/10.5194/hess-17-3205-2013

Silva, J. F. C. B. C. (2009). *Análise espacial das características hidrodinâmicas e do uso e ocupação do solo da bacia experimental do riacho Guaraíra mediante uso de geotecnologias* (Master's thesis, Universidade Federal da Paraíba). https://repositorio.ufpb.br/jspui/handle/tede/5461?mode=full

Šimůnek, J. (2015). Estimating groundwater recharge using HYDRUS-1D. *Engineering Geology and Hydrogeology*, *29*, 25–36. http://www.pc-progress.com/Documents/Jirka/Simunek_EnginGeolHydrogeol_2016.pdf

Šimůnek, J., van Genuchten, M. Th., & Šejna, M. (2008). Development and applications of the HYDRUS and STANMOD software packages and related codes. *Vadose Zone Journal*, *7*, 587–600. https://doi.org/10.2136/vzj2007.0077

Šimůnek, J., van Genuchten, M. Th., & Šejna, M. (2016). Recent developments and applications of the HYDRUS computer software packages. *Vadose Zone Journal*, *15*(7). https://doi.org/10.2136/vzj2016.04.0033

Šimůnek, J., Šejna, M., Saito, H., Sakai, M., & van Genuchten, M. Th. (2013). *The HYDRUS-1D software package for simulating the one-dimensional movement of water, heat, and multiple solutes in variably-saturated media*. PC Progress. http://www.pc-progress.com/Downloads/Pgm_hydrus1D/HYDRUS1D-4.17.pdf

Stevanato, L., Baroni, G., Cohen, Y., Fontana, C. L., Gatto, S., Lunardon, M., Marinello, F., Moretto, S., & Morselli, L. (2019). A novel cosmic-ray neutron sensor for soil moisture estimation over large areas. *Agriculture*, *9*, 202. https://doi.org/10.3390/agriculture9090202

Sutanto, S. J., Wenninger, J., Coenders-Gerrits, A. M. J., & Uhlenbrook, S. (2012). Partitioning of evaporation into transpiration, soil evaporation and interception: A comparison between isotope measurements and a HYDRUS-1D model. *Hydrology and Earth System Sciences*, *16*, 2605–2616. https://doi.org/10.5194/hess-16-2605-2012

van Genuchten, M. Th. (1980). A closed-form equation for predicting the hydraulic conductivity of unsaturated soils. *Soil Science Society of America Journal*, *44*, 892–898. https://doi.org/10.2136/sssaj1980.03615995004400050002x

van Genuchten, M. Th. (1987). *A numerical model for water and solute movement in and below the root zone*. U.S. Salinity Laboratory. http://www.pc-progress.com/Documents/RVGenugten/M1987,vG,%20Worm%20USSL%20report.pdf

van Genuchten, M.Th., & Gupta, S. K. (1993). A reassessment of the crop tolerance response function. *Journal of the Indian Society of Soil Science*, *41*, 730–737. http://www.pc-progress.com/Documents/RVGenugten/P1295.pdf

Vasconcelos, S. M. S., Teixeira, Z. A., & Alves Neto, J. (2010). Caracterização do Aquifero Jandaíra, porção situada no Estado do Ceará. *Brasil. Revista de Geologia*, *23*, 50–60. http://www.periodicos.ufc.br/geologia/article/view/1428

Ventrella, D., Castellini, M., Di Prima, S., Garofalo, P., & Lassabatère, L. (2019). Assessment of the physically-based HYDRUS-1D model for simulating the water fluxes of a Mediterranean cropping system. *Water*, *11*, 1657. https://doi.org/10.3390/w11081657

Vogel, T., van Genuchten, M. Th., & Cislerova, M. (2000). Effect of the shape of the soil hydraulic functions near saturation on variably-saturated flow predictions. *Advances in Water Resources*, *24*, 133–144. https://doi.org/10.1016/S0309-1708(00)00037-3

Wada, Y., Wisser, D., & Bierkens, M. F. P. (2014). Global modeling of withdrawal, allocation and consumptive use of surface water and groundwater resources. *Earth System Dynamics*, *5*, 15–40. https://doi.org/10.5194/esd-5-15-2014

Walker, D., Parkin, G., Schmitter, P., Gowing, J., Tilahun, S. A., Haile, A. T., & Yimam, A. Y. (2019). Insights from a multi-method recharge estimation comparison study. *Groundwater*, *57*, 245–258. https://doi.org/10.1111/gwat.12801

Wang, T., Zlotnik, V. A., Šimunek, J., & Schaap, M. G. (2009). Using pedotransfer functions in vadose zone models for estimating groundwater recharge in semiarid regions. *Water Resources Research*, *45*, 1–12. https://doi.org/10.1029/2008WR006903

Weimar, J., Köhli, M., Budach, C., & Schmidt, U. (2020). Large-scale boron-lined neutron detection systems as a 3He alternative for cosmic ray neutron sensing. *Frontiers in Water*, *2*, 16. https://doi.org/10.3389/frwa.2020.00016

Wendland, E., Barreto, C., & Gomes, L. H. (2007). Water balance in the Guarani Aquifer outcrop zone based on hydrogeologic monitoring. *Journal of Hydrology*, *342*, 261–269. https://doi.org/10.1016/j.jhydrol.2007.05.033

Wessolek, G., Duijnisveld, W. H. M., & Trinks, S. (2008). Hydropedotransfer functions (HPTFs) for predicting annual percolation rate on a regional scale. *Journal of Hydrology*, *356*, 17–27. https://doi.org/10.1016/j.jhydrol.2008.03.007

Yin, L., Hu, G., Huang, J., Wen, D., Dong, J., Wang, X., & Li, H. (2011). Groundwater-recharge estimation in the Ordos Plateau, China: Comparison of methods. *Hydrogeology Journal*, *19*, 1563–1575. https://doi.org/10.1007/s10040-011-0777-3

Yu, G., Zhuang, J., Nakayama, K., & Jin, Y. (2016). Root water uptake and profile soil water as affected by vertical root distribution. *Plant Ecology*, *189*, 15–30. https://doi.org/10.1007/sll258-006-9163-y

Zreda, M., Desilets, D., Ferré, T. P. A., & Scott, R. L. (2008). Measuring soil moisture content non-invasively at intermediate spatial scale using cosmic-ray neutrons. *Geophysical Research Letters*, *35*(21). https://doi.org/10.1029/2008GL035655

Zreda, M., Shuttleworth, W. J., Zeng, X., Zweck, C., Desilets, D., Franz, T., & Rosolem, R. (2012). COSMOS: The cosmic-ray soil moisture observing system. *Hydrology and Earth System Sciences*, *16*, 4079–4099. https://doi.org/10.5194/hess-16-4079-2012

APPENDIX A: STANDARD CORRECTIONS ON RAW NEUTRON COUNTS

The moderated neutron count rate (N in cph) measured by the CRNS has to be corrected (to N') for reference conditions (Equation A1), since neutron count rates are affected by changes in barometric air pressure, incoming neutron radiation, and atmospheric water vapor (Hawdon et al., 2014). Barometric air pressure factor (f_p, Equation A2) corrects for the atmospheric mass-shielding effect of air pressure on neutron count rate, which varies with geographic location and meteorological condition (Desilets & Zreda, 2001). Incoming neutron radiation factor (f_n, Equation A3) corrects for the strong solar activity effect on neutron count rate, normalizing the neutron count rate to a single reference solar activity level (Desilets & Zreda, 2001). Atmospheric water vapor factor (f_v, Equation A4) corrects for the effect of atmospheric hydrogen atoms on the near-ground cosmic-ray neutron mod-

eration (Rosolem et al., 2013).

$$N' = N f_{\mathrm{p}} f_{\mathrm{n}} f_{\mathrm{h}} \qquad \text{(A1)}$$

$$f_{\mathrm{p}} = e^{\left(\frac{P_i - P_{\mathrm{ref}}}{\Lambda}\right)} \qquad \text{(A2)}$$

$$f_{\mathrm{n}} = \frac{N_{\mathrm{ref}}}{N_i} \qquad \text{(A3)}$$

$$f_{\mathrm{h}} = 1 + 0.0054 \left(H_i - H_{\mathrm{ref}}\right) \qquad \text{(A4)}$$

where Λ is the mass attenuation length for high-energy neutrons (Desilets et al., 2006), calculated as 138.45 hPa from the geomagnetic cutoff rigidity map provided by Andreasen et al. (2017). P_i (in hPa) is the barometric air pressure, and P_{ref} (in hPa) is the reference air pressure baseline. N_i (in cph) is the incoming monitored neutron count rate, which was retrieved from the Potchefstroom neutron monitor in South Africa (http://www.nmdb.eu/nest/), chosen for providing a flawless time series under the closer cutoff rigidity in the Southern Hemisphere, once there was no active neutron monitor in South America; N_{ref} (in cph) is a reference monitored neutron count rate baseline. H_i (in g m^{-3}) is the absolute air humidity calculated from a relative humidity dataset, and H_{ref} (in g m^{-3}) is the air humidity baseline. The values of P_{ref}, N_{ref}, and H_{ref} were averaged on 1,001.6 hPa, 59 cph, and 18.97 g m^{-3}, respectively, for the entire period of CRNS operation, in order to smooth the effects of the strong weather seasonality on the calculation of the correction factors.

APPENDIX B: IMPLEMENTATION OF ROOT WATER UPTAKE IN HYDRUS

The actual root water uptake (RWU$_{\mathrm{a}}$) in the Richards' equation represents the root water extraction rate that is frequently assumed to be controlled by a root density exponential distribution that decreases with soil depth (Yu et al., 2016). The root water uptake can be mathematically described by macroscopic models that represent the water extraction by the matric-potential-dependent sink term RWU$_{\mathrm{a}}(h)$ (van Genuchten, 1987). This term was calculated in this study by a simplification of the equation proposed by Feddes et al. (1978), which is recommended to be used when saturated or near-saturated conditions occur for short periods (Equation B1; van Genuchten, 1987).

$$\mathrm{RWU_a}\,(h) = \frac{1}{1 + \left(\frac{h}{h_{50}}\right)^{\mathrm{p}}}\,\mathrm{RWU_p}, \text{ where } \mathrm{RWU_p} = b\,(x)\,T_{\mathrm{p}}$$
$$\text{(B1)}$$

where RWUp is the potential root water uptake, T_{p} is the potential transpiration rate, $b(x)$ is the normalized water uptake distribution, h is the water pressure head (matric potential), p is an empirical coefficient (van Genuchten & Gupta, 1993), and h_{50} is the soil water potential at which the water extraction rate is reduced by 50% from the potential rate, which can be set as -370 cm for sand soils as it has negligible effects compared to the soil hydraulic parameters (Rivera Villarreyes et al., 2014). The $b(x)$ was estimated according to Hoffman and van Genuchten (1983), adopting root depth equal to 0.70 m determined by in situ observations, which was similar to the rooting depth of xeric shrubland from northeastern Brazil during the rainy season (Pinheiro et al., 2013).